Roles Played by Toll-like Receptor-9 in Corneal Endothelial Cells after Herpes Simplex Virus Type 1 Infection

Sachiko Takeda,[1] Dai Miyazaki,[1] Shin-ichi Sasaki,[1] Yukimi Yamamoto,[1] Yuki Terasaka,[1] Keiko Yakura,[1] Satoru Yamagami,[2] Nobuyuki Ebihara,[3] and Yoshitsugu Inoue[1]

Purpose. To determine the roles played by toll-like receptor 9 (TLR9) in cultured human corneal endothelial (HCEn) cells after herpes simplex virus type 1 (HSV-1) infection and to characterize the TLR9-mediated antiviral responses.

Method. Immortalized HCEn cells were examined for TLR expression. The upregulation of inflammatory cytokines after HSV-1 infection was determined by real-time RT-PCR or protein array analyses. The TLR9-mediated HSV-1 replication was determined by real-time PCR and plaque assay. To determine whether there was an activation of the signal transduction pathway, HCEn cells that were transfected with pathway-focused transcription factor reporters were examined for promoter activity.

Results. TLR9 was abundantly expressed intracellularly in HCEn cells. The CpG oligonucleotide, a TLR9 ligand, stimulated the NF-κB activity in HCEn cells. HSV-1 infection also stimulated NF-κB and induced NF-κB -related inflammatory cytokines, including RANTES, IP-10, MCP-2, MIF, MCP-4, MDC, MIP-3α, IL-5, TARC, MCP-1, and IL-6. The induction of these cytokines was significantly reduced by blocking the activity of TLR9. In addition, viral replication in HCEn cells was significantly reduced by the inhibition of TLR9, but was preserved by a concomitant activation of the NF-κB cascade. Of the different HSV-1–induced inflammatory cascade–related transcription factors, TLR9 was found to activate NF-κB, cyclic AMP response element (CRE), and the CCAAT-enhancer-binding proteins (C/EBP) the most.

Conclusions. Corneal endothelial cells transcriptionally initiate inflammatory programs in response to HSV-1 infection related to NF-κB, CRE, and C/EBP and express arrays of inflammatory cytokine induction by TLR9. On the other hand, HSV-1 exploits TLR9-mediated NF-κB activation for its own replication. (*Invest Ophthalmol Vis Sci.* 2011;52:6729–6736) DOI:10.1167/iovs.11-7805

From the [1]Division of Ophthalmology and Visual Science, Faculty of Medicine, Tottori University, Tottori, Japan; the [2]Department of Ophthalmology, Tokyo Women's Medical University Medical Center East, Tokyo, Japan; and the [3]Department of Ophthalmology, Juntendo University School of Medicine, Tokyo, Japan.

Supported by Grant-in-Aid 20592076 and 21592258 for Scientific Research from the Japanese Ministry of Education, Science, and Culture.

Submitted for publication April 28, 2011; revised July 2, 2011; accepted July 12, 2011.

Disclosure: **S. Takeda**, None; **D. Miyazaki**, None; **S. Sasaki**, None; **Y. Yamamoto**, None; **Y. Terasaka**, None; **K. Yakura**, None; **S. Yamagami**, None; **N. Ebihara**, None; **Y. Inoue**, None

Corresponding author: Dai Miyazaki, Division of Ophthalmology and Visual Science, Faculty of Medicine, Tottori University, 36-1 Nishi-cho, Yonago, Tottori 683-8504, Japan; dm@grape.med.tottori-u.ac.jp.

The tissues of the ocular surface help maintain the clarity of the cornea and protect the eye from numerous environmental pathogens or dead cell constituents. The endothelial cells lining the inner surface of the cornea are also responsible for maintaining the optical clarity of the cornea. Because endothelial cells do not replicate in vivo, a decrease in their density can lead to blinding bullous keratopathy.[1,2]

Generally, mucosal surfaces are armed with pattern-recognition receptors (PRRs) for sensing foreign materials. The PRRs recognize various types of ligands, such as bacterial and fungal cell wall components, bacterial lipoproteins, and nucleic acids derived from bacteria, virus, and self.[3] An invasion by viruses is recognized by the toll-like receptor (TLR) family, and the recently recognized categories of intracellular PRRs that detect nucleic acids in the cytoplasm.[4] The retinoic acid-inducible gene I (*RIG-I*) and melanoma differentiation-associated gene 5 (*MDA5*) detect the RNA of pathogens. DNA-dependent activator of interferon-regulatory factors (*DAI*), absent in melanoma 2 (*AIM2*), RNA polymerase III, leucine-rich repeat flightless-interacting protein 1 (*LRRFIP1*), and interferon γ-inducible protein 16 (*IFI16*) detect intracellular DNA.

The TLRs were the first discovered and major category of PRRs. The recognition of pathogens by TLRs leads to the induction of innate immunity, inflammation, and adaptive immunity. The TLRs on the mucosal body surface function not only to keep bacteria from invading the body but also to form mutually beneficial relationships.[5] TLRs recognize commensal or pathogen-associated molecular patterns to control the function of the mucosal surface cells. For example, the TLRs regulate the proliferation of epithelial cells after intestinal injury. An absence of TLRs significantly impairs the repair of the epithelial barrier.[5] Signaling by the TLRs leads to increased inflammation and promotes the development of inflammation-associated neoplasia.[6] Thus, intricate interactions operate for the host and microbes by the many functions of the TLRs.

Corneal endothelial cells have been recently found to act as immune modulators that suppress T cell receptor-mediated $CD4^+$ T cell proliferation. They also stimulate the conversion of $CD8^+$ T cells into regulatory T cells.[7,8] These functions may contribute to the immune privilege of the eye. TLRs are especially recognized as important modulators of innate and acquired immunity. Thus, understanding how the endothelial cells behave after TLR stimulation may provide important clues on how to control immune-mediated diseases.

TLR9 is a well-known sensor of the nucleic acids of viruses and microbes. HSV-1 is the most common viral pathogen permissive to the corneal endothelial cells, and an infection by HSV-1 is manifested as herpetic keratitis. To recognize herpesvirus, the host uses a distinct repertoire of TLRs. First, the surface glycoproteins ligate to TLR2.[9,10] Second, the DNAs of herpesvirus which are rich in CpG sequences, stimulate TLR9.[11,12] And third, double-strand RNAs, generated through

Copyright 2011 The Association for Research in Vision and Ophthalmology, Inc.

self-hybridization of viral genes, activate TLR3.[13,14] TLR9 has been reported to be a crucial component in corneal epithelial cells that recognize the HSV-1 infection.[15,16] However, the roles played by TLRs in corneal endothelial cells have not been determined.

The activation of TLR9 can also cause collateral damage or exacerbation of immune-mediated diseases. For example, when self nucleic acids activate TLR9 chaperoned by anti-DNA autoantibody,[3] the TLR9 activation initiates or exacerbates autoimmune diseases.[17-19] Thus, understanding the roles played by TLR9 may help develop effective strategies to prevent unwanted inflammatory responses in the anterior chamber or corneal endothelium.

The purpose of this study was to determine the response of the TLR9 in cultured human corneal endothelial (HCEn) cells after herpes simplex virus type 1 (HSV-1) infection and to characterize the TLR9-mediated anti-viral responses. We shall show that HCEn cells express TLR9 intracellularly, and HSV-1 infection leads to the upregulation of arrays of inflammatory cytokines mediated by TLR9. Especially important was that the NF-κB cascade downstream of TLR9 can be hijacked by HSV-1 and diverted for its own replication.

Materials and Methods

Cells

An HCEn cell line was established as described in detail.[7] The HCEn cells were propagated to confluence on 6- or 96-well plates in Dulbecco's modified Eagle's medium (DMEM; Gibco, Grand Island, NY) supplemented with 10% fetal bovine serum. Primary corneal endothelial cells were obtained from the corneoscleral rims of donor eyes after the central cornea was used for keratoplasty.

The procedures used conformed to the tenets of the Declaration of Helsinki.

Viruses

Confluent monolayers of Vero cells were infected with the KOS strain of HSV-1 (generous gift from Kozaburo Hayashi, National Institutes of Health [NIH], Bethesda, MD) After 1 hour of adsorption, the medium containing the virus was aspirated, and the monolayers of cells were refed with fresh HSV-1-free medium. After attaining the maximum cytopathic effect (48-72 hours after infection), the medium was discarded, and cells with the small amount of remaining medium were frozen, thawed, and sonicated. The supernatant was collected after centrifugation at 3000 rpm for 10 minutes and overlaid onto a sucrose density gradient (10-60% wt/vol). The solution was centrifuged with a swing rotor (SW28; Beckman Instruments, Fullerton, CA) for 1 hour at 11,500 rpm. The resultant visible band at the lower part of the gradient containing the HSV-1 was washed using centrifugation at 14,000 rpm for 90 minutes and resuspended in a small volume of serum-free DMEM. The virus was then divided into aliquots and stored at −80°C until use. To infect the HCEn cells with HSV-1, the HCEn cells were adsorbed with the sucrose-density gradient purified virus stock for 1 hour at a multiplicity of infection (MOI) of 0.01 to 1, and refed with fresh medium.

Flow Cytometry

Flow cytometry was used to determine the degree of TLR expression using the following monoclonal antibodies (mAbs): TLR2 (Alexis, Plymouth Meeting, PA), TLR4 (Monosan, Uden, Netherlands), TLR3 (abCam, Cambridge, UK), and TLR9 (Oncogene, San Diego, CA). Mouse isotype IgG was used as the control. FITC-conjugated anti-mouse IgG_1 or IgG_2 (BD Pharmingen, Franklin Lakes, NJ) was used as the secondary antibody.

For flow cytometric analysis of the surface expression of TLRs on the HCEn cells, a suspension of subconfluent cells was obtained by adding 0.5% trypsin/EDTA to the HCEn cells and incubated with anti-TLR antibodies. This was followed by incubation with FITC-conjugated anti-mouse IgG (BD PharMingen). For intracellular staining of the TLRs, HCEn cell suspensions were permeabilized (Cytofix/Cytoperm; BD Biosciences) before staining. After they were washed twice in PBS, the stained cells (live-gated on the basis of the forward and side scatter profile and propidium iodide exclusion) were analyzed by flow cytometry.

Luciferase Reporter Assays

HCEn cells were transfected with luciferase reporter plasmids for AP-1, C/EBP, CRE, Elk-1, ISRE, NFAT, or NF-κB (Agilent, Santa Clara, CA). For the , internal control, HCEn cells were co-transfected with pRL-CMV (Promega, Madison, WI; using Geneporter 3000 transfection reagent; Genlantis, San Diego, CA).

For inhibition of TLR-9, TLR-9 inhibitory oligonucleotide (forward 5′-TCCTGGCGGGGAAGT-3′) (Alexis, San Diego, CA) or TLR-9 siRNA (Qiagen, Hilden, Germany) was used. For activation of the NF-κB cascade, the IκBα on the HCEn cells was inhibited by IκBα siRNA (Invitrogen, Carlsbad, CA). For transfection of siRNA, HCEn cells were transfected (RNAifect; Qiagen) 2 days after transfection of the reporter plasmids, according to the manufacturer's protocol. HCEn cells were infected with HSV-1 48 hours after siRNA transfection. The luciferase activity was measured using the dual-luciferase reporter assay system (Promega).

The target sequences of the siRNA were TLR-9 siRNA: forward 5′-CGGCAACTGTTATTACAAGAA-3′, and IκBα siRNA: forward 5′-GAGCTCCGAGACTTTCGAGGAAATA-3′.

Pharmacologic Inhibition of NF-κB Cascade

An IKK inhibitor peptide or control peptide (Merck, Darmstadt, Germany) was used to block the IκB kinase activity. The IKK inhibitor peptide contained a sequence corresponding to the active IκB phosphorylation recognition sequence. For inhibition of NF-κB p65, NF-κB p65 (Ser276) inhibitor peptide or control peptide (Imgenex, San Diego, CA) was used.

Real-Time RT-PCR

Total RNA was isolated from HSV-1-infected HCEn cells and reverse transcribed (QuantiTect Reverse Transcription Kit; Qiagen). The cDNAs were amplified and quantified on a thermal cycler (LightCycler; Roche, Mannheim, Germany) using a PCR kit (QuantiTect SYBR Green; Qiagen). The sequences of the real-time PCR primer pairs were VEGF: forward 5′-GCAGCTTGAGTTAAACGAACG-3′, reverse 5′-GGTTCCCGAAACCCTGAG-3′; IL-6: forward 5′-GATGAGTACAAAAGTCCTGATCCA-3′, reverse 5′-CTGCAGCCACTGGTTCTGT-3′; HSV-1 DNA polymerase: forward 5′-CATCACCGACCCGGAGAGGGAC-3′, reverse 5′-GGGCCAGGCGCTTGTTGGTGTA-3′; and glyceraldehyde-3-phosphate dehydrogenase (GAPDH); forward 5′-AGCCACATCGCTCAGACAC-3′, reverse 5′-GCCCAATACGACCAAATCC-3′.

To ensure equivalent loading and amplification, all products were normalized to GAPDH transcript as an internal control.

Enzyme-Linked Immunosorbent Assay

To determine the levels of secreted IL-6, supernatants collected from HSV-1-infected HCEn cells were assayed with a commercial ELISA kit (Peprotech, Rocky Hill, NJ).

For inflammatory cytokine and chemokine profiling after HSV-1 infection, supernatants were collected from HCEn cells 12 hours post infection (pi) and assayed with human cytokine antibody arrays (RayBiotech, Norcross, GA). This analysis determined the level of expression of 80 cytokines and chemokines. The intensity of the chemiluminescence signals was digitized (LAS-1000plus; Fujifilm, Tokyo, Japan, and MultiGauge software ver.2.0; Fujifilm) and normalized by using the positive control signals in each membrane.

Pathways Analysis

The set of extracted genes was analyzed for transcriptional networks of molecular events using computerized pathway analysis (Pathways Analysis 7.0; Ingenuity Systems, Redwood, CA; based on the Ingenuity Pathways Knowledge Base). The resulting networks were evaluated by the significance scores, which were expressed as the negative logarithm of the P value. The obtained score indicate the likelihood that the assembly of a set of focus genes in a network could be explained by random chance alone.

Statistical Analyses

Data are presented as the mean ± SEM. Statistical analyses were performed using t-tests or ANOVA, as appropriate.

Results

TLR9 Expression in HCEn Cells

We used flow cytometry to determine whether TLRs are expressed on HCEn cells grown in culture or primary HCEn cells, because TLRs can be expressed on the cell surface in nonhematopoietic lineage cells. No significant cell surface expression was observed (data not shown).

Next, we assessed the intracellular expression of TLRs by staining permeabilized HCEn cells and primary corneal endothelial cells. TLR9 was found to be significantly expressed intracellularly, whereas expression of TLR2, TLR3, and TLR4 was barely detectable (Fig. 1).

TLR9-Mediated NF-κB Promoter Activation in HCEn Cells after HSV-1 Infection

To determine whether the input from TLR9 is functional, we examined whether TLR9 ligand activates the NF-κB cascade, since NF-κB is the representative signaling cascade of TLR-mediated signaling. When TLR9 was stimulated with B class CpG oligonucleotide, a TLR9 ligand, there was a significant upregulation of NF-κB promoter activity, indicating that TLR9 is functional in HCEn cells (Fig. 2).

We next evaluated whether HSV-1 infection would activate the NF-κB cascade in HCEn cells and whether TLR9 plays a role in this activation. We found that HSV-1 infection significantly stimulated the promoter of NF-κB as early as 6 hours pi, and the level of expression continued to increase up to 12 hours pi (Fig. 3) The elevated NF-κB promoter activity was significantly reduced by an inhibition of TLR9. Thus, the TLR9 cascade that stimulates NF-κB is activated after HSV-1 infection.

TLR9-Mediated Inflammatory Cytokine and Chemokine Induction in HCEn Cells after HSV-1 Infection

Next, we examined whether TLR9 is involved in the induction of cytokines and chemokines in HCEn cells after HSV-1 infection. After HCEn cells were infected with HSV-1, the level of IL-6 transcript was significantly increased at 12 hours pi (i.e., the IL-6 expression relative to GAPDH was $1.4 \times 10^{-4} \pm 1.0 \times 10^{-5}$ at an HSV-1 MOI of 0.1 and $2.0 \times 10^{-6} \pm 3.1 \times 10^{-7}$ for mock infection ($P < 0.01$). The level was lower at 24 hours pi: $1.1 \times 10^{-4} \pm 4.0 \times 10^{-6}$ IL-6/GAPDH at an HSV-1 MOI of 0.1 and $2.3 \times 10^{-6} \pm 3.3 \times 10^{-7}$ for mock infection.

To examine the contribution of TLR9 to the IL-6 induction, HCEn cells treated with TLR9 inhibitory oligonucleotide were infected with HSV-1 and assessed for IL-6 induction by real-time PCR. The HSV-1 infection significantly elevated IL-6 induction at 12 hours pi (Figs. 4A, 4B). The level of IL-6 after HSV-1 infection was significantly reduced by blocking TLR9 with a TLR9 inhibitory oligonucleotide (Fig. 4A). Inhibition of TLR9 by siRNA transfection also had a similar inhibitory effect on the IL-6 induction (Fig. 4B).

We then determined whether HSV-1 infection can stimulate IL-6 secretion through TLR9. When supernatants of HSV-1-infected HCEn cells were assessed for IL-6 by ELISA, we found that HSV-1 infection significantly stimulated IL-6 secretion (Figs. 4C, 4D). This HSV-1 infection-induced IL-6 secretion was significantly suppressed by a TLR9 inhibitory oligonucleotide in a dose-dependent manner (Figs. 4C, 4D).

Next, we assessed how HSV-1 infection modulated the cytokine and chemokine milieu of HCEn cells through TLR9. Supernatants from HSV-1-infected HCEn cells were assayed for 80 cytokines and chemokines using protein array analysis and were tested for their sensitivity to TLR9 inhibition. Twenty cytokines and chemokines were significantly upregulated after HSV-1 infection, and of them,TLR9 inhibition significantly reduced the upregulation of RANTES (CCL5), IP-10 (CXCL10), MCP-2 (CCL8), MIF, MCP-4 (CCL13), MDC (CCL22), MIP-3α (CCL20), IL-5, TARC (CCL17), and MCP-1 (CCL2) (Fig. 5).

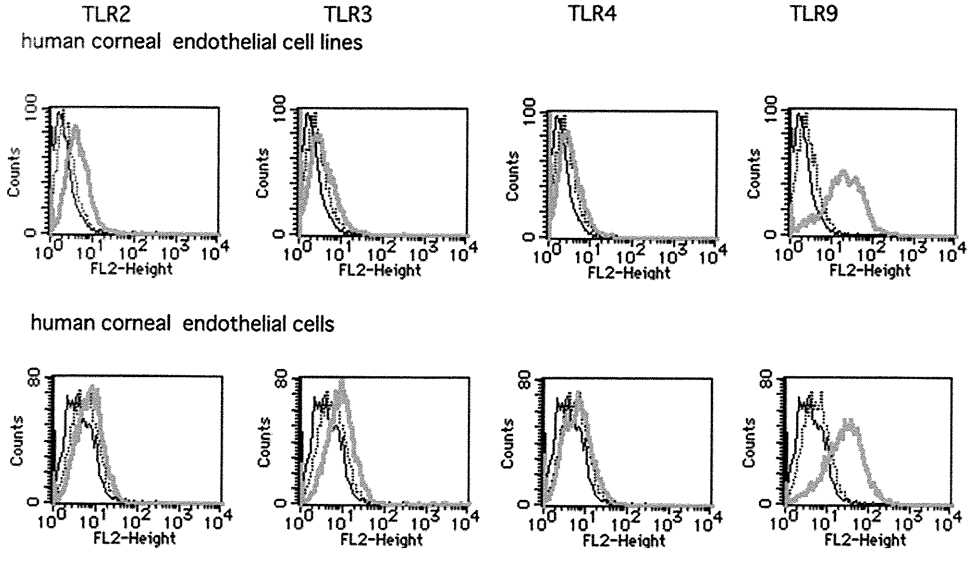

FIGURE 1. Intracellular expression of TLRs in HCEn cells. TLR 9 was significantly expressed in HCEn cells and primary human corneal endothelial cells. Expression of TLR2, -3, and -4 was barely detectable. *Solid line*: unstained; *dotted line*: control IgG stained, *gray line*: anti-TLR antibody stained.

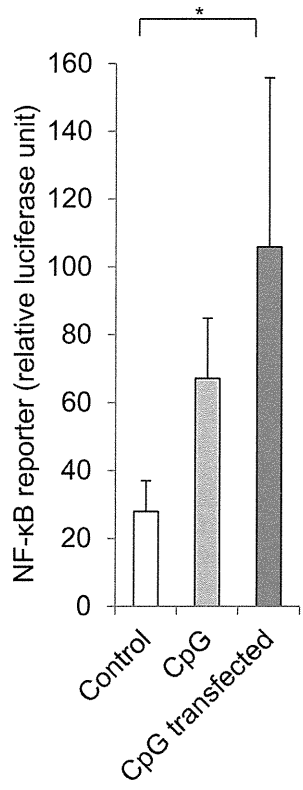

FIGURE 2. NF-κB promoter activation in HCEn cells by TLR9. HCEn cells transfected with NF-κB reporter plasmids were stimulated with CpG oligonucleotide for 24 hours and measured for luciferase activity. CpG transfection significantly elevates the NF-κB promoter activity ($n = 6$; $^*P < 0.05$).

Role of TLR9-Mediated NF-κB Activation and HSV-1 Replication

TLR9 participates in the primary defense systems against viral infection and functions to induce inflammatory cytokines after infection of HCEn cells by HSV-1. We examined whether TLR9 affects the entry and replication of HSV-1 into HCEn cells. To accomplish this, HSV-1 was adsorbed on HCEn cells, and the number of HSV-1 copies was determined by real-time PCR of HSV-1 DNA polymerase. After TLR9 was inhibited by pretreatment with TLR9 inhibitory oligonucleotide, a significant reduction in the copy number was not observed (Fig. 6A).

The contribution of TLR9 to viral replication was determined by real-time RT-PCR, and the results showed a significant reduction in the expression of the mRNA of HSV-1 DNA polymerase in HCEn cells after exposure to TLR9 inhibitory oligonucleotide (Fig. 6B). This reduction was also confirmed by titration (control oligo-treated at an MOI of 0.1: $9.3 \times 10^8 \pm 0.3 \times 10^8$; TLR9 inhibitory oligonucleotide-treated at an MOI of 0.1: $9.8 \times 10^7 \pm 0.9 \times 10^7$, $P < 0.01$).

We then assessed whether the TLR9-mediated viral replication in HCEn cells was related to NF-κB activation. The classic NF-κB cascade is regulated by IκB kinase (IKK), leading to the nuclear translocation of p65, a component of the NF-κB pathway. When HCEn cells were treated with IKK inhibitory peptide, which contained sequences corresponding to the active IκBα phosphorylation recognition sequence, the induction of HSV-1 DNA polymerase was significantly inhibited in HSV-1–infected HCEn cells (Fig. 6C). Treatment with a p65 inhibitor also significantly reduced the number HSV-1 copies (data not shown). These findings indicate that the classic NF-κB cascade is involved in HSV-1 replication in HCEn cells.

We next examined whether TLR9-inhibition–mediated suppression of HSV-1 replication can be restored by NF-κB activation. Because the activation of the classic NF-κB cascade is regulated by the degradation of IκBα, the NF-κB cascade is activated by siRNA-mediated inhibition of IκBα. Exposure to TLR9 inhibitory oligonucleotide reduced the copy number of HSV-1 DNA polymerase mRNA, and the transfection of IκBα siRNA reduced the effect of TLR9 inhibition (Fig. 6D). Collectively, these findings indicate that HSV-1 used the TLR9-mediated NF-κB activation for its own replication in HCEn cells.

Alternative Transcription Factor Activation by TLR9 in HSV-1–Infected HCEn Cells

HSV-1 infection induces an array of inflammatory cascades. This can be summarized by the transcriptional induction profiles of representative transcriptional factors. To characterize the profiles of the signaling cascades activated by HSV-1 infection and show the possible involvement of TLR9, we determined whether HSV-1 infection can activate representative transcriptional factors related to the TLR9 cascades by using transfection of reporter plasmids. The activities of transcriptional factors of cascades of NF-κB, MAPK/ERK, cAMP/PKA, MAPK/JNK, C/EBP, interferon response, and PKC/calcium were measured using reporter plasmids for NF-κB, Elk-1, cyclic AMP response element (CRE), AP-1, C/EBP, ISRE, and NFAT, respectively. HSV-1 infection significantly stimulated the transcription factors of NF-κB, Elk-1, CRE, AP-1, C/EBP, and NFAT at 24 hours pi (Fig. 7).

We then tested whether TLR9 contributes to the induction of transcription factor activities of the inflammatory cascades. When TLR9 was inhibited by siRNA transfection, the HSV-1–induced activation of CRE and C/EBP reporters was significantly reduced (Fig. 8). The other transcription factor activities, including Elk-1, AP-1, and NFAT were not appreciably affected (data not shown). Thus, HCEn cells used TLR9 leading to various types of promoter activation, including NF-κB, after HSV-1 infection.

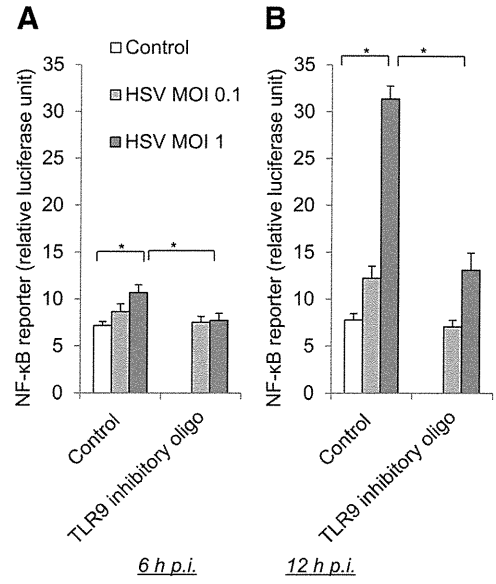

FIGURE 3. Inhibition of HSV-1 infection–induced NF-κB promoter by TLR9 inhibition. HCEn cells transfected with reporter plasmids were stimulated with HSV-1 infection for 6 (**A**) and 12 (**B**) hours, and measured for luciferase activity. Treatment by TLR9 inhibitory oligonucleotide significantly inhibited NF-κB promoter activation ($n = 6$; $^*P < 0.05$).

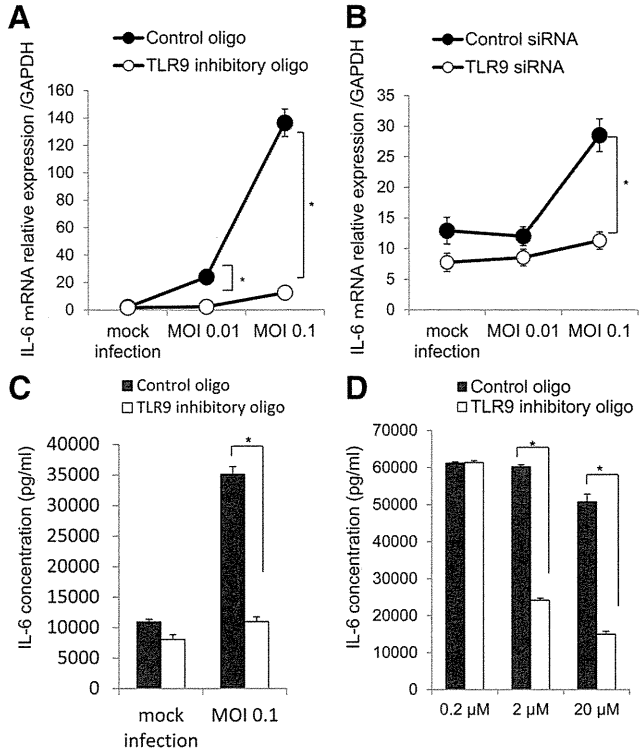

FIGURE 4. Inhibition of HSV-1 infection-induced IL-6 activation. Effect of inhibiting HSV-1 infection-induced IL-6 mRNA induction by TLR9 inhibitory oligonucleotide treatment (**A**) and by transfection of siRNA of TLR9 (**B**) at 12 hours. TLR9 blockade by inhibitory oligonucleotide or siRNA significantly reduced the HSV-1 infection-induced IL-6 mRNA activation. $n = 4$; $^*P < 0.01$. (**C**, **D**) Reduction of HSV-1 infection-induced IL-6 secretion by TLR9 blockade. TLR9 inhibitory oligonucleotide significantly reduced IL-6 secretion at 12 (**C**) and 24 (**D**) hours pi in a dose-dependent manner ($n = 6$; $^*P < 0.01$).

TLR9-Mediated Inflammatory Network after HSV-1 Infection

To summarize how HCEn cells used TLR9-mediated signals after HSV-1 infection, the TLR9-dependent cytokines induced after HSV-1 infection were analyzed for signaling interactions using a systems biological approach. Using a database of known signaling networks (Ingenuity Pathways Knowledge Base; Ingenuity Systems), we successfully generated two major biological networks with high significance scores (network 1, $P < 10^{-31}$; network 2, $P < 10^{-15}$). The most significant network was network 1, which was annotated as cell-to-cell signaling and interaction, hematologic system development and function, and immune cell trafficking, where NF-κB was centrally positioned (data not shown).

Discussion

Our results showed that TLR9 was abundantly expressed in HCEn cells and was used to initiate inflammatory responses after HSV-1 infection. HSV-1 exploited the TLR9-mediated NF-κB activation for its own replication. To resist the assault, HCEn cells transcriptionally initiate an array of inflammatory programs related to the cascades of NF-κB, ERK, MAPK (P38), JNK, cAMP/PKA, PKC, and interferon responses. Of these, TLR9 activation was especially used for the signal transduction cascades of NF-κB, CRE, C/EBP, and arrays of inflammatory cytokines, including IL-6.

In sensing microbial pathogens, conserved structural moieties are recognized by germline encoded PRRs, including the TLRs, NOD-like receptors, and C-type lectin receptors.[20] Apoptotic or necrotic cells or degradation products of the extracellular matrix, damage-associated molecules or cytokines, such as dsDNA, RNA, high-mobility group box 1 (HMGB1), ATP, hyaluronan, versican, heparin sulfate, and heat shock proteins, are abundantly present. These damage-associated molecular patterns (DAMPs) are also recognized by PRRs. Of the different PRRs, the TLRs are the most important class of receptors that are able to sense pathogen-associated molecular patterns (PAMPs). Nucleic acids, especially DNAs, are a major class of molecules that stimulate TLRs. Previously, the DNAs derived from bacteria had been considered the exclusive ligand of TLR9. However, viral genomes and self DNAs derived from necrotic or apoptotic cells have also been shown to activate TLR9. Physiologically, ligands of TLRs, including TLR9, are ubiquitous, and the corneal endothelium is continuously exposed to various components of PRR ligands. Thus, the cornea and the host are exposed to and sense the environment using combinations of PRRs. In this setting, cascades initiated from such PRRs generally converge to NF-κB or inflammasomes, where the converged signal inputs can elicit robust immune responses in synergy.[21]

For entry of HSV-1 into the host, glycoproteins, gB, gD, gH, and gL are required. For example, gB binds to paired immunoglobulin-like type 2 receptor α (PILRα) on the host.[22] gD binds to herpesvirus entry mediator (HVEM), nectin-1, or 3-O sulfated heparan sulfate, after which the host recognizes the viral invasion by the PRRs. In the TLR-mediated recognition cascade, three major molecular components—TLR2, TLR9, and TLR3—are engaged to activate innate immune responses.[23] However, the TLR-mediated interaction does not appear to affect viral entry (Fig. 6A). The sequential recognition of TLR2 and -9 that occurs after HSV-1 infection leads to a robust NF-κB activation which then induces a wide array of cytokines, chemokines, and interferons, where NF-κB plays a central role in regulating numerous cellular metabolic events. Concomitantly, HSV-1 redirects the host transcriptional machinery to

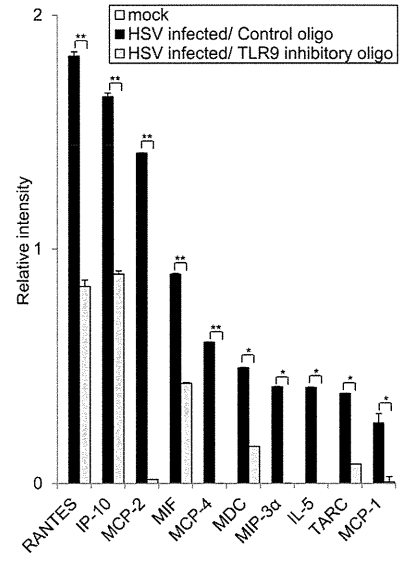

FIGURE 5. TLR9-mediated inflammatory cytokine and chemokine induction by HSV-1-infected HCEn cells. HCEn cells were adsorbed with HSV-1 at an MOI of 0.1 for 1 hour and refed with the DMEM. After 12 hours of incubation, the supernatant of HSV-1-infected HCEn cells was assayed for cytokines. TLR9-induced inflammatory cytokines and chemokines were significantly reduced by exposure to TLR9 inhibitory oligonucleotide ($n = 4$/group; $^*P < 0.05$, $^{**}P < 0.01$).

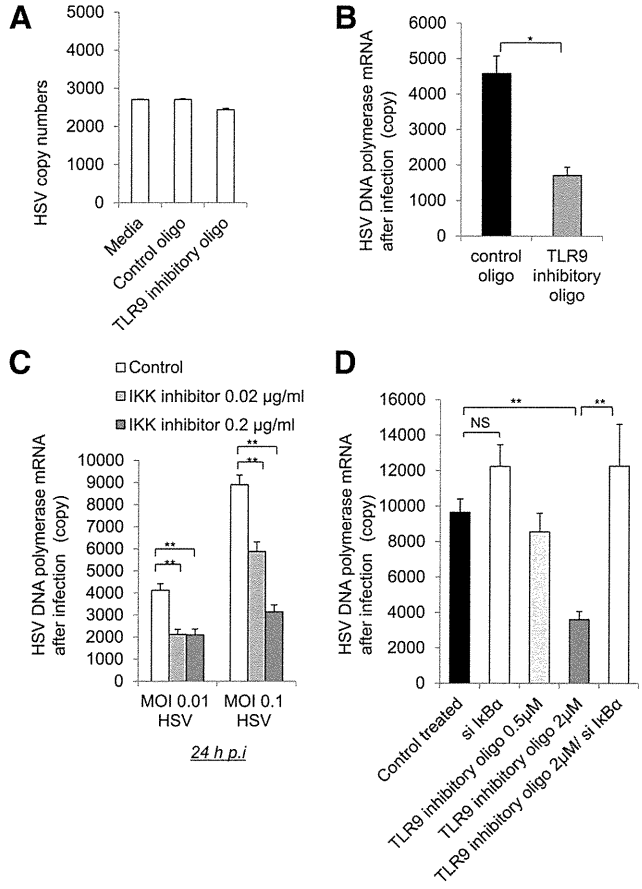

FIGURE 6. Inhibition of HSV-1 proliferation by blockade of TLR9 and NF-κB signaling cascade. (**A**) Unperturbed entry of HSV-1 into the HCEn cells by TLR9 inhibition. HSV-1 was adsorbed on HCEn cells for 1 hour. HCEn cells were washed and assessed for HSV-1 DNA polymerase copy number by using real-time PCR ($n = 8$). TLR9 inhibitory oligonucleotide did not appreciably affect HSV-1 absorption. (**B**) TLR9 inhibitory oligonucleotide impaired HSV-1 replication, shown by the reduction in copy number of HSV-1 DNA polymerase mRNA ($n = 4$, 24 hours pi). (**C**) Reduced proliferation of HSV-1 by IKK inhibitor. HCEn cells were infected with HSV-1 at the indicated MOI and assessed at 24 hours pi for copy number of HSV-1 DNA polymerase mRNA, with reverse transcription real-time PCR ($n = 4$; $P < 0.01$). (**D**) Restoration of TLR9 inhibition-mediated reduction of HSV-1 proliferation by IκBα inhibition. Treatment of TLR9 inhibitory oligonucleotide significantly reduced the copy number of HSV-1 DNA polymerase mRNA at 24 hours pi. This reduction was restored by NF-κB activation using transfection of siRNA of IκBα ($n = 4$; $^*P < 0.05$, $^{**}P < 0.01$).

express its own genes in a tightly regulated temporal cascade.[24] The three classes of genes, the immediate-early (IE) genes, including ICP-0, -4, -22, -27, and -47, followed by the early and the late genes are sequentially expressed.

To initiate productive replication of HSV-1, ICP0 plays a crucial role as a strong activator of all classes of HSV-1 genes and a propagator of lytic infections. ICP0 possesses NF-κB-binding elements on its promoter. The transcription of ICP0 is dependent on activation of NF-κB of the host, which is triggered by the recruitment of p65/RelA.[24] Inhibition of the NF-κB cascade, including the inhibition of IKK or dominant negative IκBα, significantly suppresses viral replication (Fig. 6).[24–26] Very recently, the UL31 of HSV-1 was also shown to be necessary for optimal NF-κB activation and expression of ICP4, ICP8, and glycoprotein C.[27]

The use of host NF-κB for viral replication is not limited to HSV-1 because NF-κB-binding sites are also located in the genome of different members of the herpes virus family.[28,29] Moreover, HSV-1 is equipped with the ability to effectively block multiple innate signaling for its survival. For example, virion host shutoff protein (VHS) degrades the host mRNA by its RNase function, US11 or γ34.5 inhibits PKR (RNA-activated protein kinase), and ICP47 inhibits MHC class I loading.[30–37] After the viral replication is completed, ICP-0 directs the inhibition of inflammatory responses by ubiquitin-specific peptidase 7 (USP7) translocation, which leads to the inhibition of NF-κB and JNK.[30] Thus, HSV-1 hijacks and exploits the crucial components of the host immune system, TLR9 and NF-κB, for its own use.

There are two major signaling pathways for TLR: NF-κB and MAPKs. In the MAPK cascade, the JNK, p38, and ERK pathways are conventionally activated, leading to the activation of AP-1, CRE, Elk-1, and C/EBP elements in the promoters. In addition, the C/EBP family of transcription factors is involved in many biological functions, including regulating cytokine expression, proliferation, and tumor progression.[38–40] We found that the reporter activity of NF-κB, CRE, and C/EBP are activated by TLR9 after HSV-1 infection. Analysis of the HSV-1 infection-induced transcriptome of HCEn cells showed strong inductions of CREBBP and C/EBPα, which are representative transcription factors related to CRE and C/EBP.

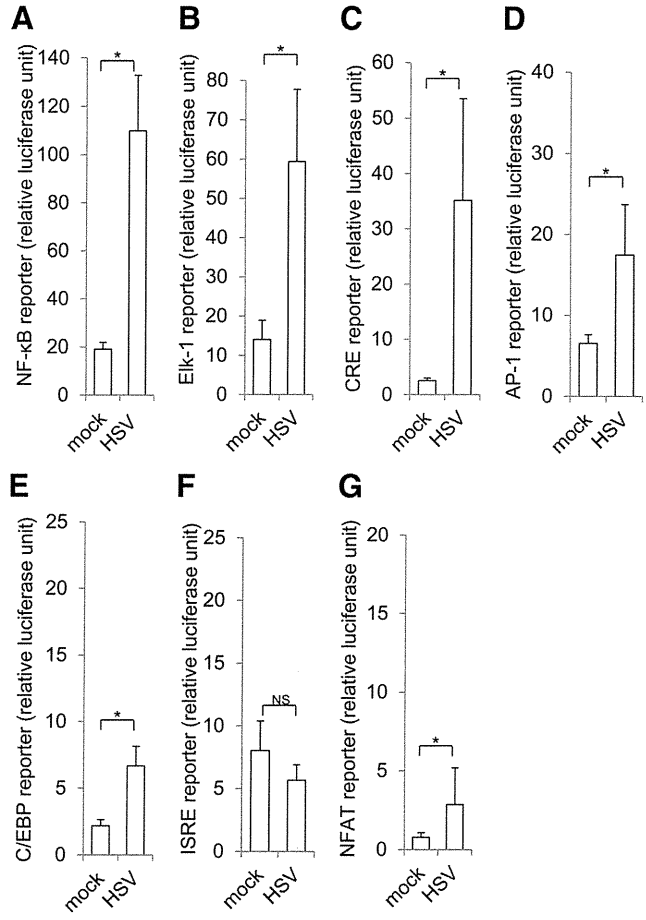

FIGURE 7. Signaling cascade-focused promoter activation in HCEn cells by HSV-1 infection. HCEn cells transfected with reporter plasmids were stimulated with HSV-1 infection for 24 hours at an MOI of 0.1 and measured for luciferase activity for (**A**) NF-κB, (**B**) Elk-1, (**C**) CRE, (**D**) AP-1, (**E**) C/EBP, (**F**) ISRE, and (**G**) NFAT. HSV-1 infection significantly elevated promoter activities of NF-κB, ELK-1, CRE, AP-1, C/EBP, and NFAT ($n = 6$; $^*P < 0.05$).

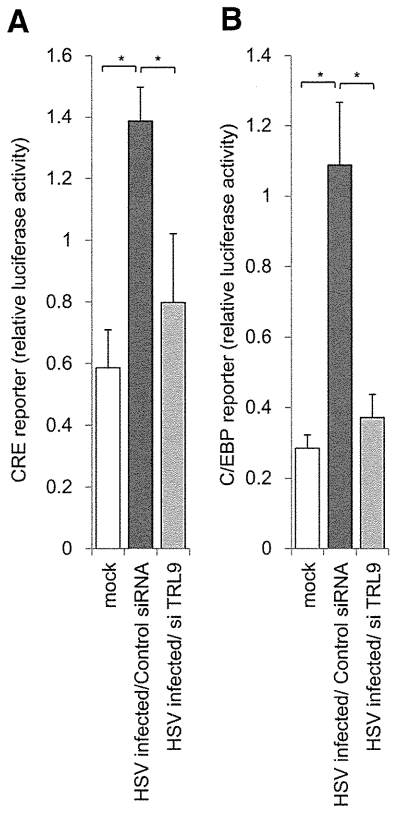

FIGURE 8. Inhibition of HSV-1 infection-induced CRE and C/EBP promoter activation by TLR9 inhibition. HCEn cells transfected with reporter plasmids were infected with HSV-1 at an MOI of 0.1 and measured for luciferase activity at 12 hours pi. Transfection of siRNA of TLR9 significantly inhibited the reporter activities of CRE (**A**) and C/EBP (**B**). ($n = 6$; $^*P < 0.05$).

Generally, transcriptional activation is regulated by different levels of transcriptional factor activation and interactions. On infection by *Helicobacter pylori*, the AP-1 and CRE elements in the cyclooxygenase promoter are activated by TLR2 and -9.[41] In TLR-mediated activation of IL-6 and TNF-α, both NF-κB and C/EBP binding elements in the promoter are critical for their transcriptional activation.[42–44] In HSV-1-infected HCEn cells, TLR9 input activated the NF-κB signal transduction cascade (Fig. 3), and our bioinformatic analysis of the induced cytokines and chemokines which are sensitive to TLR9 inhibition, were summarized as NF-κB-dependent inflammatory cascade. However, the NF-κB cascade may not be sufficient to fully explain the transcriptional activation of inflammatory cytokines. In HCEn cells, the activations of CRE, C/EBP, and NF-κB were involved in the TLR9-mediated signaling cascade (Fig. 8) and presumably in the TLR9-mediated induction of inflammatory cytokines and chemokines. At least two of the recognition sequences of these transcription factors exist in the promoters of TLR responsive cytokines and chemokines (data not shown). This may explain the unexpectedly wide array of inflammatory cytokines that was inhibited by TLR9 suppression.

We used immortalized HCEn cells as models of corneal endothelial cells in situ. The HCEn cells have similar capabilities as primary corneal endothelial cells and organ cultured corneal endothelial cell in inducing representative cytokines including MCP-1, IL-6, IL-8, CXCL2, TGFβ2, and thrombospondin 1.[8,45] However, there is still some question of whether immortalized HCEn cells can truly reflect the in vivo properties of corneal endothelial cells such as HSV-1 infection-induced endotheliitis. For this, in vivo analysis may help in gaining a better understanding of the physiological roles of the endothelial cells during a viral infection.

At present, a murine model of HSV-1-induced corneal endotheliitis is not available. We used the KOS strain for this study because our initial hypothesis was based on the findings of our earlier studies.[46,47] Very recently, the KOS strain has been reported to have a mutation of the *US8A* gene and defective *US9* gene.[48] *US9* is especially involved in neuronal virulence. However, a defective *US9* does not appear to affect the cell-to-cell spread in permissive epithelial cells.[49] In addition, no apparent dysfunction was reported for the elongated US8A by mutation.

To summarize, corneal endothelial cells express TLR9 intracellularly to recognize dsDNAs and HSV-1 infection. HSV-1 usurps this TLR-mediated NF-κB activation for its own replication.

Acknowledgments

The authors thank Duco Hamasaki for editing this article.

References

1. Murphy C, Alvarado J, Juster R, Maglio M. Prenatal and postnatal cellularity of the human corneal endothelium: a quantitative histologic study. *Invest Ophthalmol Vis Sci.* 1984;25:312–322.
2. Miyata K, Drake J, Osakabe Y, et al. Effect of donor age on morphologic variation of cultured human corneal endothelial cells. *Cornea.* 2001;20:59–63.
3. Barton GM, Kagan JC. A cell biological view of Toll-like receptor function: regulation through compartmentalization. *Nat Rev Immunol.* 2009;9:535–542.
4. Paludan SR, Bowie AG, Horan KA, Fitzgerald KA. Recognition of herpesviruses by the innate immune system. *Nat Rev Immunol.* 2011;11:143–154.
5. Abreu MT. Toll-like receptor signalling in the intestinal epithelium: how bacterial recognition shapes intestinal function. *Nat Rev Immunol.* 2010;10:131–144.
6. Xiao H, Gulen MF, Qin J, et al. The Toll-interleukin-1 receptor member SIGIRR regulates colonic epithelial homeostasis, inflammation, and tumorigenesis. *Immunity.* 2007;26:461–475.
7. Sugita S, Usui Y, Horie S, et al. Human corneal endothelial cells expressing programmed death-ligand 1 (PD-L1) suppress PD-1+ T helper 1 cells by a contact-dependent mechanism. *Invest Ophthalmol Vis Sci.* 2009;50:263–272.
8. Yamada Y, Sugita S, Horie S, Yamagami S, Mochizuki M. Mechanisms of immune suppression for CD8+ T cells by human corneal endothelial cells via membrane-bound TGFbeta. *Invest Ophthalmol Vis Sci.* 2010;51:2548–2557.
9. Sarangi PP, Kim B, Kurt-Jones E, Rouse BT. Innate recognition network driving herpes simplex virus-induced corneal immunopathology: role of the toll pathway in early inflammatory events in stromal keratitis. *J Virol.* 2007;81:11128–11138.
10. Kurt-Jones EA, Chan M, Zhou S, et al. Herpes simplex virus 1 interaction with Toll-like receptor 2 contributes to lethal encephalitis. *Proc Natl Acad Sci U S A.* 2004;101:1315–1320.
11. Lund J, Sato A, Akira S, Medzhitov R, Iwasaki A. Toll-like receptor 9-mediated recognition of Herpes simplex virus-2 by plasmacytoid dendritic cells. *J Exp Med.* 2003;198:513–520.
12. Krug A, Luker GD, Barchet W, Leib DA, Akira S, Colonna M. Herpes simplex virus type 1 activates murine natural interferon-producing cells through toll-like receptor 9. *Blood.* 2004;103:1433–1437.
13. Jacquemont B, Roizman B. RNA synthesis in cells infected with herpes simplex virus, X: properties of viral symmetric transcripts and of double-stranded RNA prepared from them. *J Virol.* 1975;15:707–713.
14. Weber F, Wagner V, Rasmussen SB, Hartmann R, Paludan SR. Double-stranded RNA is produced by positive-strand RNA viruses and DNA viruses but not in detectable amounts by negative-strand RNA viruses. *J Virol.* 2006;80:5059–5064.

15. Hayashi K, Hooper LC, Chin MS, Nagineni CN, Detrick B, Hooks JJ. Herpes simplex virus 1 (HSV-1) DNA and immune complex (HSV-1-human IgG) elicit vigorous interleukin 6 release from infected corneal cells via Toll-like receptors. *J Gen Virol.* 2006;87: 2161-2169.
16. Hayashi K, Hooper LC, Detrick B, Hooks JJ. HSV immune complex (HSV-IgG: IC) and HSV-DNA elicit the production of angiogenic factor VEGF and MMP-9. *Arch Virol.* 2009;154:219-226.
17. Boule MW, Broughton C, Mackay F, Akira S, Marshak-Rothstein A, Rifkin IR. Toll-like receptor 9-dependent and -independent dendritic cell activation by chromatin-immunoglobulin G complexes. *J Exp Med.* 2004;199:1631-1640.
18. Leadbetter EA, Rifkin IR, Hohlbaum AM, Beaudette BC, Shlomchik MJ, Marshak-Rothstein A. Chromatin-IgG complexes activate B cells by dual engagement of IgM and Toll-like receptors. *Nature.* 2002;416:603-607.
19. Christensen SR, Kashgarian M, Alexopoulou L, Flavell RA, Akira S, Shlomchik MJ. Toll-like receptor 9 controls anti-DNA autoantibody production in murine lupus. *J Exp Med.* 2005;202:321-331.
20. Chen GY, Nunez G. Sterile inflammation: sensing and reacting to damage. *Nat Rev Immunol.* 2010;10:826-837.
21. Napolitani G, Rinaldi A, Bertoni F, Sallusto F, Lanzavecchia A. Selected Toll-like receptor agonist combinations synergistically trigger a T helper type 1-polarizing program in dendritic cells. *Nat Immunol.* 2005;6:769-776.
22. Wang J, Fan Q, Satoh T, et al. Binding of herpes simplex virus glycoprotein B (gB) to paired immunoglobulin-like type 2 receptor alpha depends on specific sialylated O-linked glycans on gB. *J Virol.* 2009;83:13042-13045.
23. Reske A, Pollara G, Krummenacher C, Katz DR, Chain BM. Glycoprotein-dependent and TLR2-independent innate immune recognition of herpes simplex virus-1 by dendritic cells. *J Immunol.* 2008;180:7525-7536.
24. Amici C. Herpes simplex virus disrupts NFκ-B regulation by blocking its recruitment on the IκB promoter and directing the factor on viral genes. *J Biol Chem.* 2006;281:7110-7117.
25. Gregory D, Hargett D, Holmes D, Money E, Bachenheimer SL. Efficient replication by herpes simplex virus type 1 involves activation of the IκB kinase-IκB-p65 pathway. *J Virol.* 2004;78:13582-13590.
26. Amici C, Belardo G, Rossi A, Santoro MG. Activation of I kappa b kinase by herpes simplex virus type 1: a novel target for antiherpetic therapy. *J Biol Chem.* 2001;276:28759-28766.
27. Roberts KL, Baines JD. UL31 of herpes simplex virus 1 is necessary for optimal NF-kappaB activation and expression of viral gene products. *J Virol.* 2011;85:4947-4953.
28. Rong BL, Libermann TA, Kogawa K, et al. HSV-1-inducible proteins bind to NF-kappa B-like sites in the HSV-1 genome. *Virology.* 1992;189:750-756.
29. Cherrington JM, Mocarski ES. Human cytomegalovirus ie1 transactivate the alpha promoter-enhancer via an 18-base-pair repeat element. *J Virol.* 1989;63:1435-1440.
30. Daubeuf S, Singh D, Tan Y, et al. HSV ICP0 recruits USP7 to modulate TLR-mediated innate response. *Blood.* 2009;113:3264-3275.
31. Murphy JA, Duerst RJ, Smith TJ, Morrison LA. Herpes simplex virus type 2 virion host shutoff protein regulates alpha/beta interferon but not adaptive immune responses during primary infection in vivo. *J Virol.* 2003;77:9337-9345.
32. Poppers J, Mulvey M, Khoo D, Mohr I. Inhibition of PKR activation by the proline-rich RNA binding domain of the herpes simplex virus type 1 Us11 protein. *J Virol.* 2000;74:11215-11221.
33. He B, Gross M, Roizman B. The gamma(1)34.5 protein of herpes simplex virus 1 complexes with protein phosphatase 1alpha to dephosphorylate the alpha subunit of the eukaryotic translation initiation factor 2 and preclude the shutoff of protein synthesis by double-stranded RNA-activated protein kinase. *Proc Natl Acad Sci U S A.* 1997;94:843-848.
34. Fruh K, Ahn K, Djaballah H, et al. A viral inhibitor of peptide transporters for antigen presentation. *Nature.* 1995;375:415-418.
35. Hill A, Jugovic P, York I, et al. Herpes simplex virus turns off the TAP to evade host immunity. *Nature.* 1995;375:411-415.
36. Eidson KM, Hobbs WE, Manning BJ, Carlson P, DeLuca NA. Expression of herpes simplex virus ICP0 inhibits the induction of interferon-stimulated genes by viral infection. *J Virol.* 2002;76: 2180-2191.
37. Melroe GT, DeLuca NA, Knipe DM. Herpes simplex virus 1 has multiple mechanisms for blocking virus-induced interferon production. *J Virol.* 2004;78:8411-8420.
38. Tanaka T, Akira S, Yoshida K, et al. Targeted disruption of the NF-IL6 gene discloses its essential role in bacteria killing and tumor cytotoxicity by macrophages. *Cell.* 1995;80:353-361.
39. Screpanti I, Romani L, Musiani P, et al. Lymphoproliferative disorder and imbalanced T-helper response in C/EBP beta-deficient mice. *EMBO J.* 1995;14:1932-1941.
40. Lu YC, Kim I, Lye E, et al. Differential role for c-Rel and C/EBP / in TLR-mediated induction of proinflammatory cytokines. *J Immunol.* 2009;182:7212-7221.
41. Chang YJ, Wu MS, Lin JT, Chen CC. Helicobacter pylori-Induced invasion and angiogenesis of gastric cells is mediated by cyclooxygenase-2 induction through TLR2/TLR9 and promoter regulation. *J Immunol.* 2005;175:8242-8252.
42. Pope RM, Leutz A, Ness SA. C/EBP beta regulation of the tumor necrosis factor alpha gene. *J Clin Invest.* 1994;94:1449-1455.
43. Dendorfer U, Oettgen P, Libermann TA. Multiple regulatory elements in the interleukin-6 gene mediate induction by prostaglandins, cyclic AMP, and lipopolysaccharide. *Mol Cell Biol.* 1994;14: 4443-4454.
44. Wedel A, Sulski G, Ziegler-Heitbrock HW. CCAAT/enhancer binding protein is involved in the expression of the tumour necrosis factor gene in human monocytes. *Cytokine.* 1996;8:335-341.
45. Yamagami H, Yamagami S, Inoki T, Amano S, Miyata K. The effects of proinflammatory cytokines on cytokine-chemokine gene expression profiles in the human corneal endothelium. *Invest Ophthalmol Vis Sci.* 2003;44:514-520.
46. Terasaka Y, Miyazaki D, Yakura K, Haruki T, Inoue Y. Induction of IL-6 in transcriptional networks in corneal epithelial cells after herpes simplex virus type 1 infection. *Invest Ophthalmol Vis Sci.* 2010;51:2441-2449.
47. Miyazaki D, Haruki D, Takeda D, et al. Herpes simplex virus type 1-induced transcriptional networks of corneal endothelial cells indicate antigen presentation function. *Invest Ophthalmol Vis Sci.* 2011;52:4282-4293.
48. Negatsch A, Mettenleiter TC, Fuchs W. Herpes simplex virus type 1 strain KOS carries a defective US9 and a mutated US8A gene. *J Gen Virol.* 2011;92:167-172.
49. Wang F, Tang W, McGraw HM, Bennett J, Enquist LW, Friedman HM. Herpes simplex virus type 1 glycoprotein e is required for axonal localization of capsid, tegument, and membrane glycoproteins. *J Virol.* 2005;79:13362-13372.

Amino Acid Profiles in Human Tear Fluids Analyzed by High-Performance Liquid Chromatography and Electrospray Ionization Tandem Mass Spectrometry

MINA NAKATSUKASA, CHIE SOTOZONO, KAZUTAKA SHIMBO, NOBUKAZU ONO, HIROSHI MIYANO, AKIRA OKANO, JUNJI HAMURO, AND SHIGERU KINOSHITA

• PURPOSE: To identify the 23 amino acid profiles in human tear fluids, and to evaluate whether the ocular disease conditions reflect the amino acid profiles.

• DESIGN: Laboratory investigation.

• METHODS: We evaluated the concentrations and relative composition of 23 amino acids in tear fluids obtained from 31 healthy volunteers using reversed-phase high-performance liquid chromatography and electrospray ionization tandem mass spectrometry, and compared them with those in plasma and aqueous humor. We also evaluated the tear-fluid amino acid profiles from 33 affected subjects.

• RESULTS: The amino acid profiles of the basal tear and reflex tear were found to be similar, and 4 distinct groups of healthy volunteers (male, female, young, and elderly) showed similar profiles. Absolute concentrations of taurine (Tau) and L-glutamine were significantly dominant in these tear fluids. The relative compositions of Tau, L-glutamic acid, L-arginine (Arg), and citrulline in the tear fluid were significantly higher than those in the plasma and aqueous humor. Analysis of the hierarchical clustering of the amino acid profiles clearly distinguished severe ocular surface diseases from non–ocular surface diseases. The relative compositions of Tau, L-methionine, and Arg decreased in severe ocular surface disease subjects compared with non–ocular surface disease subjects.

• CONCLUSIONS: Tear-fluid amino acid profiles differ from those in plasma and aqueous humor. Steady-state tear-fluid amino acid profiles might reflect ocular-surface homeostasis and the observed changes of amino acids might have a close relation with the disease conditions on the ocular surface. (Am J Ophthalmol 2011;151:799–808. © 2011 by Elsevier Inc. All rights reserved.)

Accepted for publication Nov 1, 2010.

From the Department of Ophthalmology, Kyoto Prefectural University of Medicine, Kyoto, Japan (M.N., C.S., J.H., S.H.); the Life Science Research Laboratories, AJINOMOTO Co, Inc, Kawasaki, Japan (K.S., H.M.); and the Pharmaceutical Research Laboratories, AJINOMOTO Co, Inc, Kawasaki, Japan (N.O., A.O.).

Inquiries to Shigeru Kinoshita, Department of Ophthalmology, Kyoto Prefectural University of Medicine, 465 Kajii-cho, Hirokoji-agaru, Kawaramachi-dori, Kamigyo-ku, Kyoto 602-0841, Japan; e-mail: shigeruk@koto.kpu-m.ac.jp

METABOLISM CAN BE VIEWED AS A NETWORK that can adapt to various nutritional conditions and that may become disturbed during disease and physiologic insults. Specific variations in amino acid profiles in blood have been reported in the context of liver failure,[1] renal failure,[2] cancer,[3] diabetes,[4] and so on. Conventionally, amino acid has long been considered a source of protein synthesis in the nutritional term, and the existence of a free amino acid supply to the tissues plays a pivotal role in maintaining organ and body protein homeostasis.[5] However, besides their role as substrates for protein synthesis, amino acids have multiple and critical functions, not only in maintaining baseline steady-state homeostasis, but also in the pathophysiology of diverse human disorders. It is now widely accepted that changes in amino acid availability have profound effects on many aspects of cellular functions, including the regulation of cell signaling, gene expression, and the transport of amino acids themselves.[6–8] For example, the pathophysiologic relevance of L-glutamine (Gln, GluNH2), L-arginine (Arg), and L-leucine (Leu) have been implicated in severely traumatized patients,[9] in the inflammatory response,[10] and in activating the mammalian target of rapamycin (mTOR).[11,12]

Tear fluids provide oxygen and other nutrients, as well as chemical mediators including antimicrobial and immunologic mediators. Considering the relevance of amino acids and glucose in the homeostatic metabolism of tissues, the profound understanding of the function of amino acid in tear fluids is as crucial as that of chemical mediators. Previously, a few reports have presented contradicting results on the amount of a limited number of amino acids in human tears.[13,14] The existence of a significantly higher concentration of L-valine (Val), L-isoleucine (Ile), and L-histidine (His) has been reported, and with the exception of L-aspartate (Asp), L-glutamic acid (Glu), and taurine (Tau), the quantities found in tears were at a comparable level with those found in plasma.[13,14]

Today, amino acid profiles for biological specimens are commonly analyzed by ion-exchange chromatography, a method in which amino acids and related compounds can be measured.[12,15] Recently, a new method for rapidly analyzing amino acids was developed that involves derivatization with a novel reagent, followed by reversed-phase

0002-9394/$36.00
doi:10.1016/j.ajo.2010.11.003

© 2011 BY ELSEVIER INC. ALL RIGHTS RESERVED.

high-performance liquid chromatography and electrospray ionization tandem mass spectrometry (HPLC/ESI-MS/MS).[16] Now, more than 100 different analytes with amino groups can be measured within 10 minutes by the combination of the precolumn derivatization and HPLC/ESI-MS/MS techniques. This method represents an alternative to traditional amino acid analysis techniques. The aim of this study was to reveal and describe the amino acid profiles in human tear fluids since this new method now makes it possible to analyze samples in trace amounts (below 0.5 μL) and with a superior reproducibility.[16] In addition, the possible physiological and pharmacologic function of amino acids will be discussed.

METHODS

• NORMAL VOLUNTEER SUBJECTS: Enrolled in this study were normal volunteer subjects with no corneal-, conjunctival-, or lacrimal-system abnormalities as assessed by slit-lamp examination. Free amino acids were evaluated in blood samples obtained from 11 healthy young male (mean age: 22.9 ± 1.4 years), 6 healthy young female (mean age: 21.0 ± 0.7 years), 6 healthy elderly male (mean age: 69.5 ± 3.8 years), and 11 healthy elderly female (mean age: 71.5 ± 4.0 years) volunteer subjects. Basal tear samples were collected from the young and elderly subjects (n = 31; young male: 10; young female: 6; elderly male: 6; elderly female: 9) and reflex tear samples were also collected from the young subjects (n = 16; male: 10; female: 6). Basal and reflex tear fluid samples (0.5−1.0 μL) were collected from the inferior tear meniscus of each subject using a microcapillary tube. Reflex-tear stimulation was initiated by inserting an applicator into the nose of each subject. Aqueous humor samples were obtained from the elderly subjects (n = 16; male: 6; female: 10) through the use of a 1-mL syringe with a 30-gauge needle prior to cataract surgery, and all of the obtained samples were free of contamination by blood fluids.

• PREPARATION OF TEAR FLUID AND AQUEOUS HUMOR SAMPLES: Each tear sample was transferred into a 0.5-mL sterile microfuge tube and then centrifuged. Supernatants were stored at –70°C until assaying for the amino acid levels. After thawing, 0.5 μL of each tear sample was diluted with 4.5 μL of sterile purified water, and then extracted by the addition of 20 μL of acetonitrile and mixing with a vortex mixer. The samples were centrifuged at 10 000 rpm for 1 minute, and the supernatants were then analyzed. A quantity of 1.0 μL of aqueous humor was used for each sample, with the same dilution as that of the tear fluid.

• PATIENTS WITH OCULAR SURFACE DISEASE AND CORNEAL OR SCLERAL DISEASE: Tear samples were collected from 33 affected subjects composed of 18 subjects with severe ocular surface diseases and 15 subjects with corneal or scleral diseases. Severe ocular surface diseases included Stevens-Johnson syndrome (SJS) (n = 10), chemical injury (n = 4), thermal burn (n = 2), and stem cell deficiency from an unknown cause (n = 2). The corneal or scleral diseases of the other 15 subjects included granular dystrophy (n = 2), band-shaped keratopathy (n = 2), keratoconus (n = 2), bullous keratopathy (n = 2), lattice dystrophy (n = 1), corneal erosion (n = 1), postcorneal infection (n = 2), necrotizing keratitis (n = 1), and scleritis (n = 2). Those 15 subjects were all classified as non–ocular surface disease.

• BIOCHEMICAL ASSAYS OF TEAR FLUID AMINO ACID AND AQUEOUS HUMOR AMINO ACID: For measurement of the amino acid concentration in the tear fluid and aqueous humor samples, we adopted precolumn derivatization with AccQ·Tag (Waters Corporation, Milford, Massachusetts, USA) to increase the ionization efficiency of the adducts before being analyzed by the multiple-reaction monitoring mode of reversed-phase HPLC HP1100 series (Agilent Technologies, Inc, Palo Alto, California, USA) and triple quadrupole tandem mass spectrometry (API4000 LC/MS/MS system; Applied Biosystems, Inc, Foster City, California, USA).[16–18] For derivatization with 20 μL of AccQ·Tag reagent, 20 μL of a deproteinized tear sample was added to 60 μL of 0.2-M borate buffer (pH 8.8) and then heated at 55°C for 10 minutes. The reaction mixture was diluted with 100 μL of 0.2% acetic acid and 5 μL of the mixture was then injected onto the HPLC column (L-Column, 50 mm × 2.0 mm, 3-μm particles; Chemicals Evaluation and Research Institute, Tokyo, Japan) prior to MS detection at a flow rate of 0.25 mL/min.

• BIOCHEMICAL ASSAYS OF PLASMA AMINO ACID: The plasma was separated and deproteinized in a final concentration of 3% sulfosalicylic acid. All samples were stored at –70°C until measurement using HPLC (SRL Inc, Tokyo, Japan). The basic amino acid and related molecules (23 compounds) were measured and used in the analysis. Those compounds are as follows: L-tyrosine (Tyr), Val, Leu, L-methionine (Met), Ile, Gln, L-serine (Ser), L-lysine (Lys), L-asparagine (Asn, AspNH2), L-threonine (Thr), L-alanine (Ala), Glu, His, L-ornithine (Orn), L-cystine (Cys2), L-proline (Pro), L-tryptophan (Trp), Arg, Tau, glycine (Gly), citrulline (Cit), Asp, and L-phenylalanine (Phe).

• STATISTICAL ANALYSIS: Statistical analysis was performed using SPSS statistical analysis software (SPSS Inc, Chicago, Illinois, USA). Hierarchical clustering analysis was performed using JMP7.0 software (SAS Institute, Inc, Cary, North Carolina, USA). The correlations among 23 amino acid concentrations as well as

TABLE 1. Concentration (Mean ± SEM, μM) of Each Amino Acid in the Basal Tears, Reflex Tears, Aqueous Humor, and Plasma of Normal Subjects

	Basal Tear (n = 31)	Reflex Tear (n = 16)	Aqueous Humor (n = 16)	Plasma (n = 34)
Gly	10.7 ± 2.8	14.4 ± 7.1	0.4 ± 0.1	231.3 ± 11.1
Ala	23.8 ± 4.8	19.5 ± 8.5	14.4 ± 2.7	385.5 ± 14.5
Val	3.5 ± 0.9	3.8 ± 1.4	6.7 ± 1.1	244.7 ± 8.5
Leu	10.1 ± 1.9	6.4 ± 1.9	3.3 ± 0.6	125.4 ± 6.1
Ile	1.1 ± 0.3	1.1 ± 0.5	1.5 ± 0.3	68.7 ± 3.6
Ser	14.4 ± 4.2	26.4 ± 13.0	3.9 ± 0.8	113.6 ± 3.3
Thr	5.4 ± 1.2	8.4 ± 3.6	3.5 ± 0.7	127.6 ± 3.8
Met	2.4 ± 0.1	2.2 ± 0.1	0.9 ± 0.2	28.1 ± 1.3
AspNH2 (Asn)	1.4 ± 0.3	1.5 ± 0.7	1.0 ± 0.2	49.6 ± 1.5
GluNH2 (Gln)	42.1 ± 6.8	25.4 ± 6.3	28.7 ± 5.2	589.5 ± 11.0
Pro	8.4 ± 1.4	6.7 ± 1.5	0.5 ± 0.1	180.2 ± 8.5
Phe	10.7 ± 1.9	5.7 ± 1.5	2.8 ± 0.5	63.7 ± 2.0
Tyr	1.3 ± 0.5	1.1 ± 0.5	2.8 ± 0.6	73.5 ± 3.8
Trp	7.1 ± 0.7	6.6 ± 1.0	0.9 ± 0.1	52.9 ± 1.8
Asp	13.2 ± 4.5	18.2 ± 11.6	0.0 ± 0.0	1.8 ± 0.2
Glu	30.2 ± 4.8	20.9 ± 4.8	0.1 ± 0.0	42.3 ± 2.8
Lys	5.7 ± 1.2	3.5 ± 1.2	3.1 ± 0.6	195.7 ± 7.2
Arg	18.7 ± 1.6	14.4 ± 2.5	2.5 ± 0.5	82.7 ± 3.0
His	1.9 ± 0.7	3.2 ± 1.9	1.5 ± 0.3	83.7 ± 2.0
Cit	10.1 ± 0.8	8.2 ± 1.5	1.2 ± 0.2	35.1 ± 1.7
Orn	3.3 ± 1.1	7.1 ± 3.0	0.4 ± 0.1	79.3 ± 4.9
Cys2	1.0 ± 0.2	0.6 ± 0.2	0.3 ± 0.1	49.0 ± 2.4
Tau	195.1 ± 26.9	100.1 ± 18.7	1.2 ± 0.3	57.7 ± 2.0

Ala = L-alanine; Arg = L-arginine; Asp = L-aspartate; AspNH2 (Asn) = L-asparagine; Cit = citrulline; Cys2 = L-cystine; Glu = L-glutamic acid; GluNH2 (Gln) = L-glutamine; Gly = glycine; His = L-histidine; Ile = L-isoleucine; Leu = L-leucine; Lys = L-lysine; Met = L-methionine; Orn = L-ornithine; Phe = L-phenylalanine; Pro = L-proline; Ser = L-serine; Tau = taurine; Thr = L-threonine; Trp = L-tryptophan; Tyr = L-tyrosine; Val = L-valine.

among plasma and/or ophthalmic fluid (basal tear, reflex tear, and aqueous humor) samples were clustered using the Ward method. For the red>gray>blue color system, the depth in the red color or blue color reflected the different degree of values above or below the mean (gray color), respectively. Graphic presentations of box plots were generated using R (R Foundation for Statistical Computing, Vienna, Austria). In each box plot, the top and bottom of the boxes were the first and third quartiles, respectively, and the length of the box represented the inter-quartile range within 50% of the values that were included. The horizontal line within each box represented the median, the vertical lines showed the largest/smallest observation that fell within a distance of 1.5 times the box size from the nearest quartile in the box, and the additional points were considered "extreme" values and are shown separately.

These presentations and analyses were performed based on each of the absolute amino acid concentrations (μM) or relative amino acid composition (percentage), calculated by each amino acid concentration/total 23 amino acid concentrations.

RESULTS

• COMPARISON OF AMINO ACID PROFILES AMONG TEAR FLUID, AQUEOUS HUMOR, AND PLASMA SAMPLES OF NORMAL SUBJECTS: Amino acid concentrations in a trace amount of tear fluids of 0.5 to 1.0 μL were able to be measured reproducibly by HPLC/ESI-MS/MS. The reproducibility of the measurements was confirmed in separate experiments using normal tear fluids. The Table shows the concentrations of each amino acid in the basal tear, the reflex tear, the aqueous humor, and the plasma of normal subjects. A significant difference of amino acid profiles between the tear fluid, the aqueous humor, and the plasma samples was confirmed. The concentration of total amino acids in the tear fluid samples (means ± SEM: 382.1 ± 42.6 μM) was lower than that in the plasma samples (2961.6 ± 63.1 μM) but higher than that in the aqueous humor samples (81.6 ± 15.2 μM). Ala, Val, and Gln were dominant components in the plasma samples (more than 240 μM). Gly, Pro, and Lys were also major components in the plasma samples.

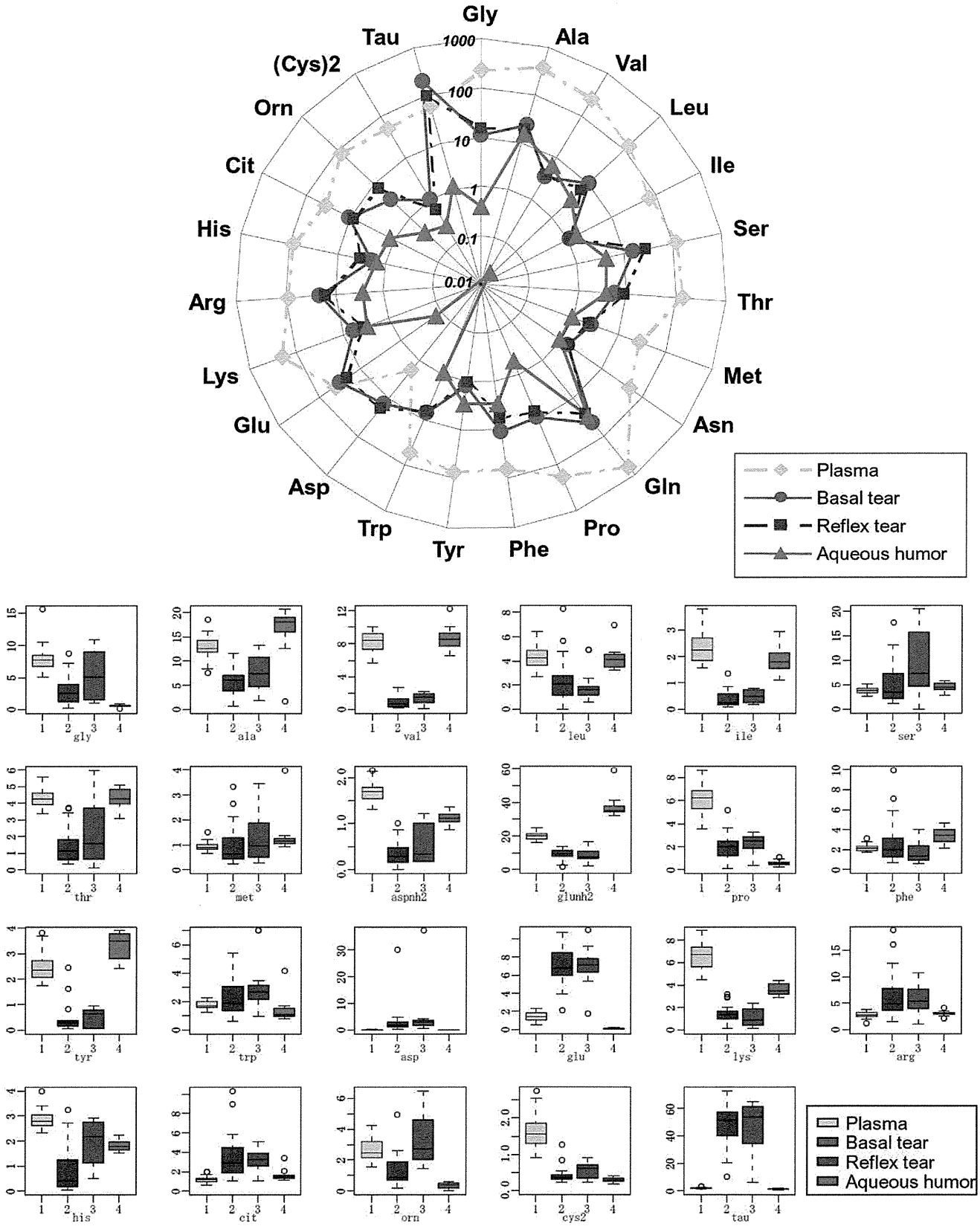

FIGURE 1. The differences of amino acid profiles of normal subjects between basal tear, reflex tear, and aqueous humor samples, compared with that of plasma samples. (Top) Mean values of 23 amino acid concentrations (μM) of basal tear (n = 31) (blue), reflex tear (n = 16) (purple), aqueous humor (n = 16) (red), and plasma (n = 34) (green) samples from normal subjects are shown in

In the tear fluids, Tau, Glu, and Gln were dominant components (more than 25 μM). Arg and Cit were of a higher concentration than other amino acid concentrations, whereas Val, Ile, Met, Asn, Tyr, His, and Orn were of a lower concentration (below 5 μM) (Table, and Figure 1, Top). Notably, the concentrations of Tau and Glu were significantly higher than (3.4 times higher) or comparable with (0.7 times higher) those in plasma samples. Asp also was of a higher value than that in plasma samples. The amino acid concentrations and profiles of the basal tear fluid and reflex tear fluid were found to be similar.

Since it has been shown that the metabolomic profiling of amino acid can be helpful in revealing specific physiological conditions or states, and that the ratios between some specific amino acids can be useful in diagnosing them,[19] we performed some analyses based on not only amino acid concentrations but also relative amino acid composition (Figure 1, Bottom). The composition of amino acid in aqueous humors was rather analogous to that in plasmas, although the levels of Gly, Pro, and Orn were low. In the tear fluid samples, Tau and Glu were of a higher relative amino acid composition (25.0 times higher and 4.9 times higher, respectively; $P < .001$) (Tukey test) than those in the plasma samples, yet the aqueous humor samples were not (Tau: 0.73 times higher, Glu: 0.09 times higher). The relative compositions of Arg and Cit in the tear fluid samples were smaller but statistically significantly higher than those in the plasma and aqueous humor samples. There was no significant difference between the basal tear fluid and reflex tear fluid in 23 relative amino acid compositions (Tukey test).

In an aim to build up a simple visual presentation, the correlations among 23 amino acid concentrations and the relative amino acid composition of 31 basal tear fluid, 16 reflex tear fluid, 16 aqueous humor, and 34 plasma samples were clustered (Figure 2). Plasma samples were clearly clustered at the highest position, followed by tear fluid samples and then aqueous humor samples.

• COMPARISON OF TEAR-FLUID AMINO ACID PROFILES AMONG YOUNG AND ELDERLY VOLUNTEERS: The change of amino acid concentration attributable to aging is known to exist in other body fluids.[20] In this study, a preliminary analysis was carried out on the basal tear fluid and plasma samples of adults that differed by both age and sex. The mean values of 23 amino acids in relation to concentration and composition that were obtained from young male (n = 10), young female (n = 6), elderly male (n = 6), and elderly female (n = 9) normal subjects were examined. The Tukey test showed that the differences were not statistically significant. Hierarchical clustering charts of both the concentration and composition did not exhibit any distinct clustering trends among these 4 groups (data not shown).

• DISTINCTIVE CHANGE OF AMINO ACID PROFILES IN TEAR FLUIDS FROM DISEASED EYES: The difference of amino acid concentrations and profiles among tear fluids from individuals of severe ocular surface disease and non–ocular surface disease was investigated. Means of the 23 amino acid concentrations (μM) from severe ocular surface disease (n = 18) and non–ocular surface disease (n = 15) were shown in a radar chart (Figure 3, Top). The concentrations of amino acid were highly elevated in tear fluids from severe ocular surface disease subjects compared with those from non–ocular surface disease subjects. Four amino acids (Val, Ile, Tyr, and Glu) showed a significant P value of less than .01, and 15 amino acids showed a P value of less than .05 (Student t test). Of important note is the fact that the changes were not restricted to the concentration, but also extended to the amino acid profile, namely composition.

Next, the distribution pattern of the amino acid composition in tear fluids from the severe ocular surface disease subjects was compared with those from the non–ocular surface disease subjects. Amino acid composition (%) of tear fluids from 15 non–ocular surface disease subjects (column 1, left) and 18 severe ocular surface disease subjects (column 2, right) are shown in the box plots (Figure 3, Bottom). The significant changes were the decrease in Arg, Met, and Tau and the increase in Orn, Lys, and Thr in the severe ocular surface disease subjects.

Analysis of the hierarchical clustering of the amino acid profiles of tear fluids from severe ocular surface disease subjects and non–ocular surface disease subjects indicated clear clustering of 12 of the 18 specimens from individuals with severe ocular surface disease when classified on the basis of amino acid composition (Figure 4). Interestingly, the composition-based clustering exhibited 5 distinctive clusters of amino acid, namely Tau/Met/Arg, Asn/Tyr/Val/Ile/Lys, Glu/Gln, Cit/Leu/Phe/Trp/Pro, and Asp/His/Thr/Orn/Ser/Gly/Ala. Decreased amino acid, Tau, Met, and Arg were included in 1 cluster, which suggests a correlation of the metabolism and/or transport of these amino acids in inflammatory eyes.

DISCUSSION

IN THIS STUDY, WE PERFORMED THE SYSTEMATIC QUANTIFICATION of free amino acids in human tear fluids by HPLC/ESI-MS/

the radar chart. (Bottom) Amino acid composition data (percentages) from plasma (n = 34) (green), basal tear (n = 31) (blue), reflex tear (n = 16) (purple), and aqueous humor (n = 16) (red) samples are shown in the box plots. The box represents the first and third quartiles, and the horizontal line within each box represents the median. The vertical lines show the largest/smallest observation, and the additional points are "extreme" values.

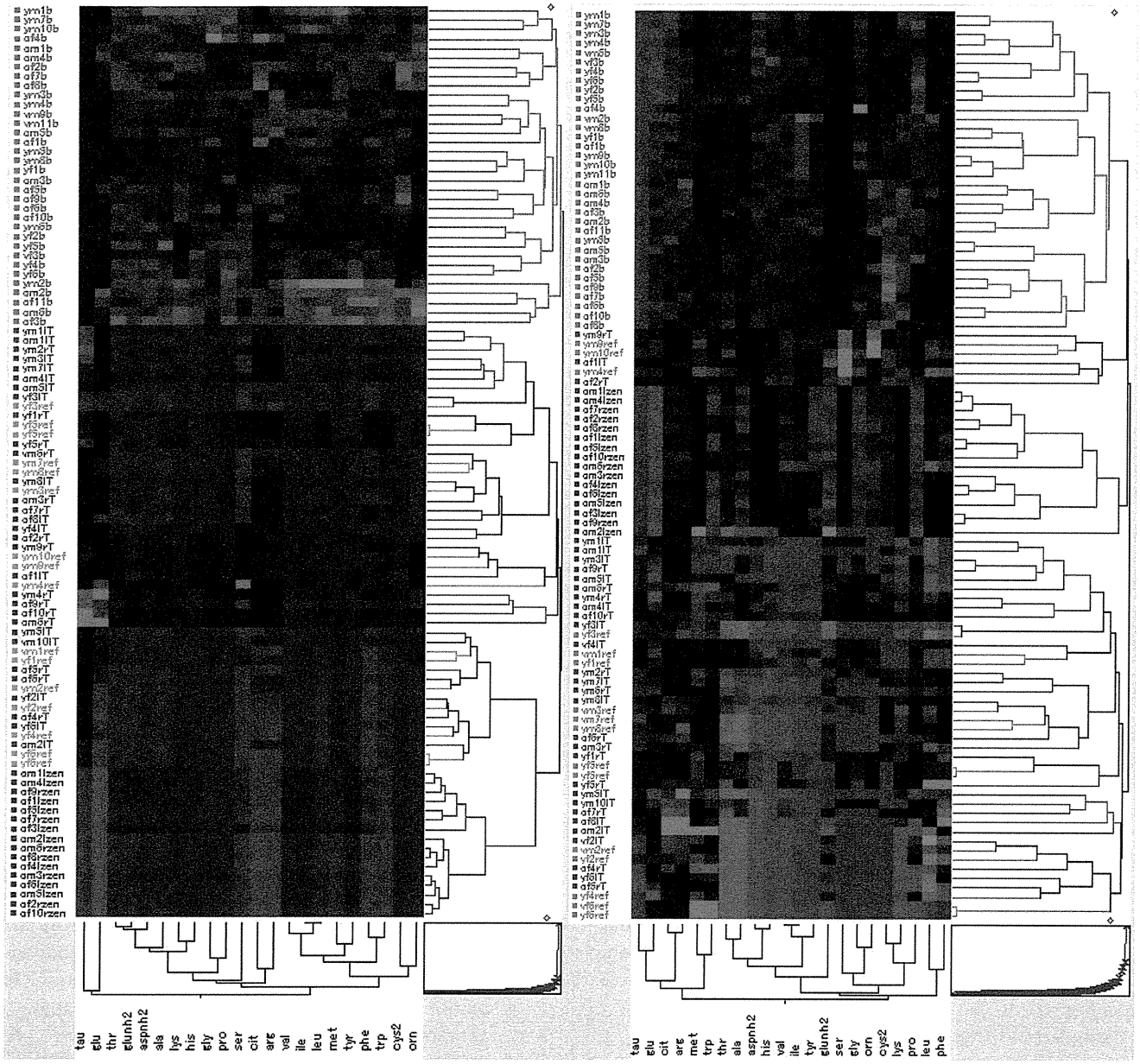

FIGURE 2. Hierarchical clustering of the amino acid profiles of basal tear, reflex tear, aqueous humor, and plasma samples of normal subjects. The correlations among 23 amino acid concentrations (Left) and relative amino acid compositions (Right) of basal tear (n = 31) (blue), reflex tear (n = 16) (green), aqueous humor (n = 16) (purple), and plasma (n = 34) (red) samples were clustered using the Ward method.

MS. The amino acid profiles showed the following characteristics: 1) the amino acid profiles in tear fluids differ from those in aqueous humors and plasmas, 2) the absolute concentrations of Tau, Glu, and Asp in tear fluids are significantly higher than, or comparable with, those in plasma samples, 3) the amino acid profile in the aqueous humor samples was rather analogous to that in the plasma samples, 4) the amino acid profiles of the tear fluid of distinct groups (male vs female, young vs elderly) are similar, and 5) amino acid profiles of tear fluids from severe ocular surface disease subjects differed from those of non–ocular surface disease subjects.

The combination of the precolumn derivatization and HPLC/ESI-MS/MS techniques enabled the analysis of 120 body fluid samples in a single day and may possibly provide an alternative to traditional techniques used for amino acid analysis. From this viewpoint, we theorize that our high-speed, reliable procedure for amino acid analysis will prove to be a useful technique for the diagnosis and management of inherited disorders of amino acid metabolism in the clinical setting. In this study, we discovered that almost all amino acids exist in tear fluid. The plasma concentration of amino acid is the sum of its rates of appearance in and disappearance from plasma, and amino acid appearance

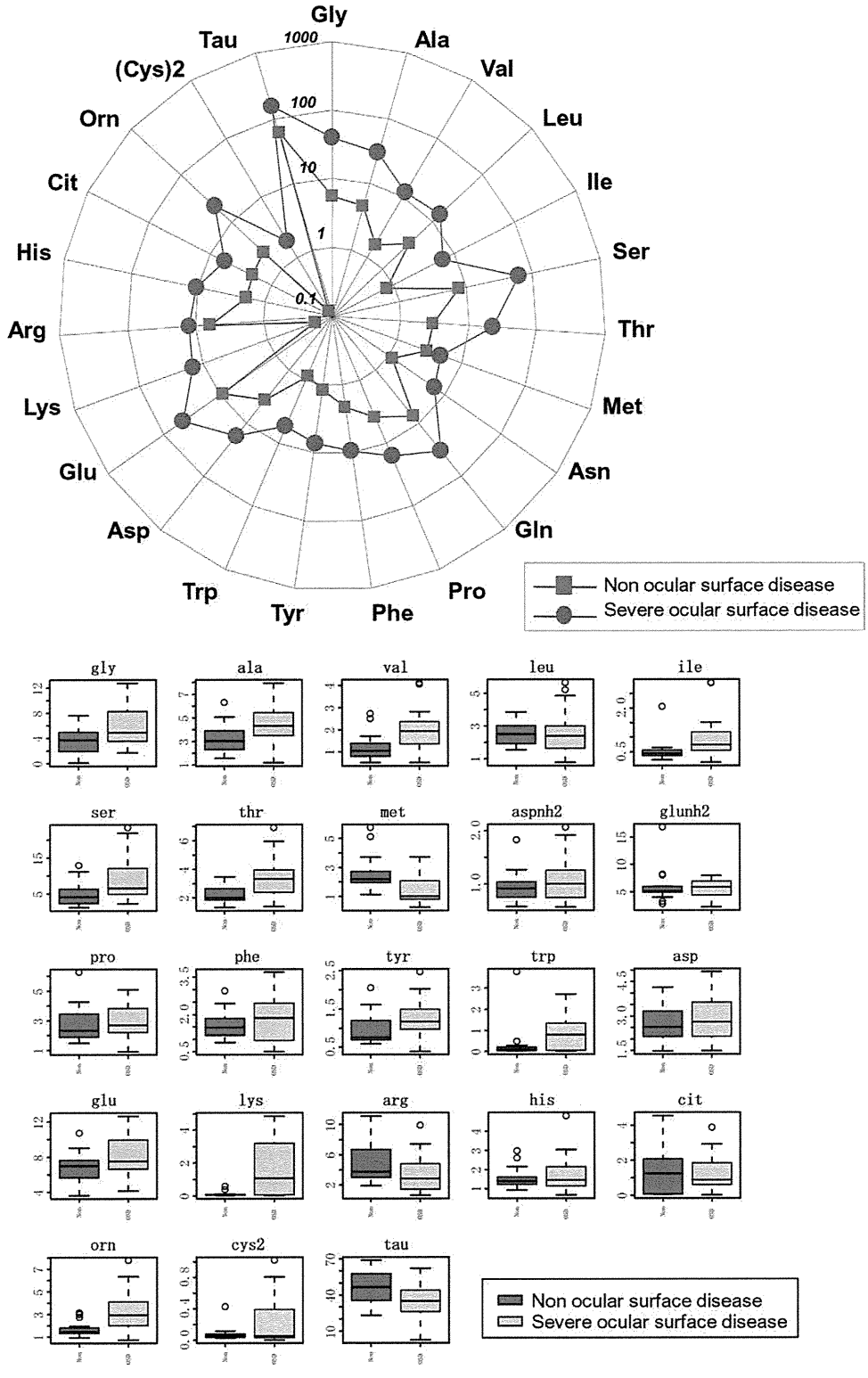

FIGURE 3. The differences of amino acid concentrations between tear fluids from severe ocular surface disease subjects and non–ocular surface disease subjects. (Top) Means values of 23 amino acid concentrations (μM) of tears from severe ocular surface disease subjects (n = 18) (blue) and non–ocular surface disease subjects (n = 15) (red) are shown in the radar chart. (Bottom) Amino acid composition data (percentages) of tears from non–ocular surface disease (n = 15) (red; left) and severe ocular surface disease (n = 18) (blue; right) subjects are shown in the box plots.

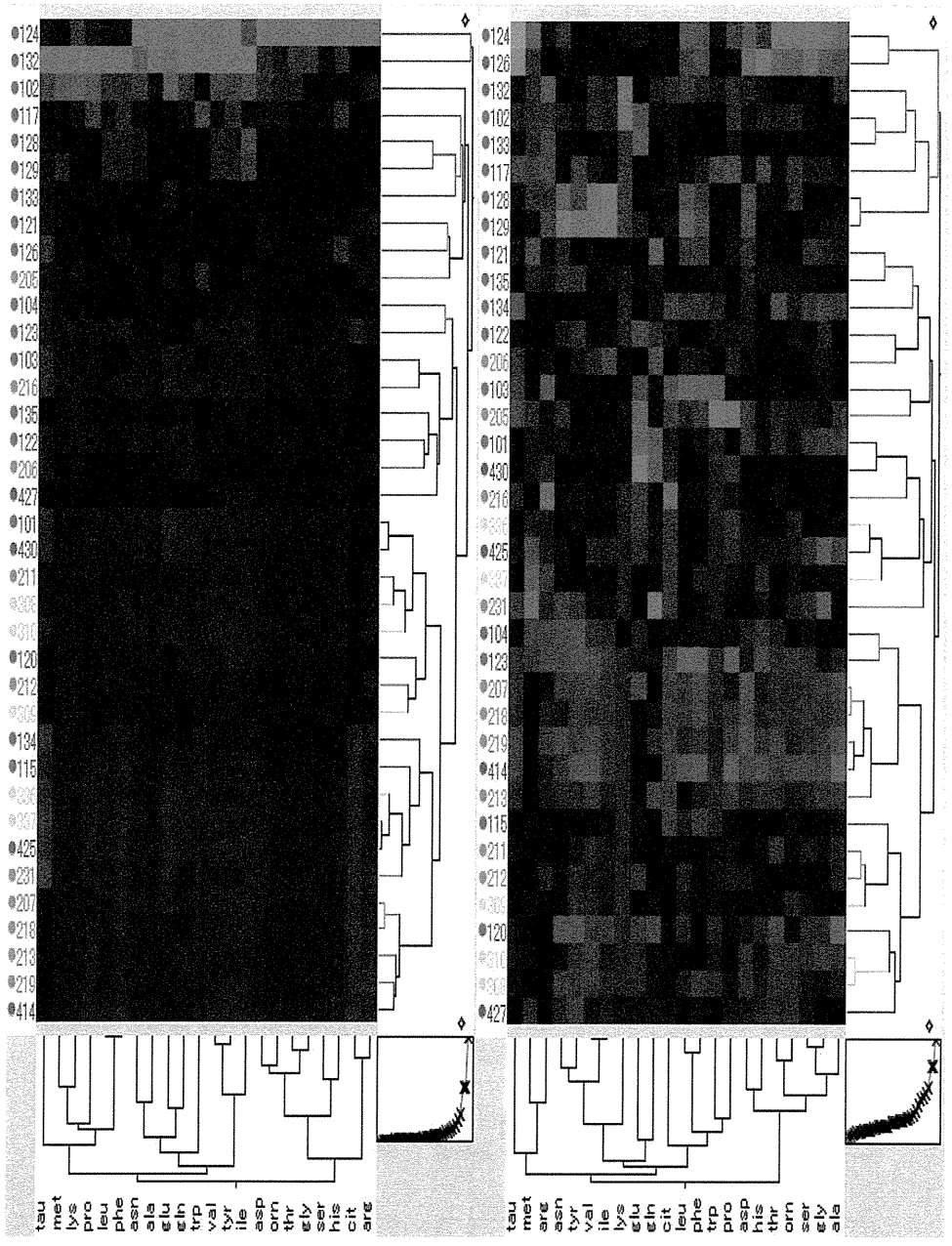

FIGURE 4. Hierarchical clustering of the amino acid profiles of tear fluids from severe ocular surface disease subjects and non–ocular surface disease subjects. The correlations among 23 amino acid concentrations (Left) and relative amino acid compositions (Right) of tear samples from severe ocular surface disease subjects (n = 18) (red) and non–ocular surface disease subjects (n = 15) (green) were clustered using the Ward method. The concentrations and relative composition of 23 amino acids in tear fluids differ from those in plasma and aqueous humor. Analysis of the hierarchical clustering of the amino acid profiles distinguished severe ocular surface diseases from non-ocular surface diseases. Steady-state tear-fluid amino acid profiles might reflect ocular-surface homeostasis and the observed changes of amino acids might have a close relation with the disease conditions on the ocular surface.

and disappearance are tightly regulated. In some circumstances, tissue uptake of amino acid and further metabolism depend on plasma amino acid concentrations. Mere determinations of plasma amino acid concentrations at the basal state (ie, postabsorptive) provide a rather limited amount of information.[21]

Previously, a few reports have presented contradicting results on the amount of limited kinds of free amino acids in human tears.[13,14] In those studies, the quantities found in tear fluids were at a comparable level with those found in plasma, except for the levels of Asp, Glu, and Tau. The high level for Tau in tear fluids was reported previously,[14] and Tau has been identified as a major player in numerous biological functions[22,23] and is involved in the regulation of the proinflammatory responses.[22] Very

recently, it has been demonstrated that Tau plays a key role in regulating epithelial barrier function.[24] In this study, the concentration of Tau was confirmed to be very high in the tear fluid samples compared with that in the plasma samples, consistent with the previous reports. These findings signal the necessity to discriminate the subtle function of Tau under physiological and pathologic environments. Plasma Tau levels are usually high, although decreases are observed in response to surgical injury and numerous pathologic conditions, including cancer and sepsis.[25] The observed higher concentration of Glu (and probably that of Asp as well) may reflect the energy demand at the luminal side of corneal/conjunctival epithelial cells. Mucosal tissue exhibits a high rate of aerobic glycolysis, and in intestinal metabolism, luminal Gln, Glu, and Asp, but not glucose, has been found to contribute critically to the respiratory CO_2 produced in this tissue.[26] Although considered nonessential, Gln becomes conditionally essential during severe catabolic stress in which intracellular and plasma Gln levels decrease rapidly.[27–29]

It is very difficult to discuss with clarity the underlying mechanism for the regulation of amino acid profiles in tear fluids, because to date, almost no information has been presented on the dynamic roles of ocular surface epithelial cells in regard to amino acid transportation. The presence of the Na^+-dependent neutral amino acid transporter has been reported in a rabbit primary corneal epithelial cell culture and rabbit corneas.[30] Whether all or part of the amino acid component of tear fluids is attributable to secretion, filtration, local synthesis, or local degradation of proteins is unknown. However, it is speculated that the amino acids are transported from tear fluids into the corneal tissues by this transport system. It is important to discuss the characteristic variance of amino acid profiles in tear fluid between the individuals with and without ocular surface disease. Diseases that develop because of the loss of corneal epithelial stem cells are known as limbal stem cell deficiency. Among limbal stem cell deficiency, SJS, ocular cicatricial pemphigoid, and severe chemical or thermal burns are known as severe ocular surface disease, because these diseases are intractable, even with corneal epithelial transplantation, and visual prognosis is poor. In cases of severe ocular surface disease, corneal neovascularization, ingrowth of fibrous tissue, and stromal scarring occur and often progress with chronic inflammation. However, the mechanisms of chronic inflammation and pathophysiology are still unclear. In this study, both the concentrations and relative composition of the amino acids differed between the severe ocular surface disease subjects and the non–ocular surface disease subjects. Hierarchical clustering on the amino acid profiles of tears clearly distinguished severe ocular surface disease subjects from non–ocular surface disease subjects. Surprisingly, hierarchical clustering also distinguished the eyes with SJS at the chronic stage as severe ocular surface disease, in which at least clinically, no inflammation and no scarring were detected. Amino acid profiles might be a sensitive marker of ocular surface inflammation, or they may be a new method to reflect ocular surface pathologic dynamics.

It is well known that supplemental Arg promotes wound healing following trauma shock. The major catabolic products of Arg are Orn and Cit. Because of the competition between nitric oxidase synthase and arginase for the same substrate Arg, their activities are regulated reciprocally. As for conditionally essential amino acids, Arg exhibited a significant decrease with a moderate decrease in Cit in the eyes with severe ocular surface disease, while Orn exhibited a prominent increase, indicating the possible polarization of tissue inflammation to the axis of arginase (oxidative tissue regeneration).[31–34] In this context, the reason why the increased composition of Orn over Cit, reflecting the high arginase activity, exists only in the tear fluids of individuals with chronic ocular surface inflammation is a subject that requires further investigation.

We can now harness information buried in amino acid profiles for the generation of diagnostic and surrogate markers. The methods described in this study might be applicable to the clinical setting and prove useful in diagnosing various physiologic and disease states at the ocular surface. Our results using cluster analysis of amino acid profiles in tear fluids suggest that the analysis can help us understand the complex interrelations that make up the metabolism of the ocular surface. In the future, a far more stringent study with controlled background factors will need to be performed to solidify the present observations. Amino acid represents a convenient set of metabolites that can be easily measured. Once the association of abnormalities in individual amino acid concentrations and/or composition with specific ocular surface diseases or physiologic conditions has been addressed, amino acid profiles for the generation of diagnostic and surrogate markers may prove to help advance biomedical and nutritional science in the field of ocular physiology.

PUBLICATION OF THIS ARTICLE WAS SUPPORTED IN PART BY HEALTH AND LABOR SCIENCES RESEARCH GRANTS (RESEARCH ON Intractable Diseases) from the Ministry of Health, Labour and Welfare of Japan, Tokyo, Japan, and the Japanese Ministry of Education, Culture, Sports, Science and Technology, Tokyo, Japan; a research grant from the Kyoto Foundation for the Promotion of Medical Science, Kyoto, Japan; and the Intramural Research Fund of Kyoto Prefectural University of Medicine, Kyoto, Japan. The authors indicate no financial conflict of interest. Involved in conception and design (C.S., J.H., S.K.); analysis and interpretation (M.N., C.S., K.S., N.O., H.M., J.H.); writing the article (M.N., C.S., A.O., J.H.); critical revision of the article (C.S., J.H., S.K.); final approval of the manuscript (M.N., C.S., K.S., N.O., H.M., A.O., J.H., S.K.); data collection (M.N., C.S.); provision of materials, patients, or resources (M.N., C.S.); statistical expertise (N.O., A.O.); obtaining funding (C.S., S.K.); and literature search (M.N., C.S., J.H.). All experimental procedures were approved by the Institutional Review Board for Human Studies at Kyoto Prefectural University of Medicine (KPUM). Prior informed consent was obtained from all patients, and this study was performed in accordance with the tenets of the Declaration of Helsinki for research involving human subjects.

REFERENCES

1. Holm E, Sedlaczek O, Grips E. Amino acid metabolism in liver disease. Curr Opin Clin Nutr Metab Care 1999;2(1): 47–53.
2. Hong SY, Yang DH, Chang SK. The relationship between plasma homocysteine and amino acid concentrations in patients with end-stage renal disease. J Ren Nutr 1998;8(1): 34–39.
3. Watanabe A, Higashi T, Sakata T, Nagashima H. Serum amino acid levels in patients with hepatocellular carcinoma. Cancer 1984;54(9):1875–1882.
4. Watanabe A, Takei N, Hayashi S, Nagashima H. Serum neutral amino acid concentrations in cirrhotic patients with impaired carbohydrate metabolism. Acta Med Okayama 1983;37(4):381–384.
5. Broer S. Amino acid transport across mammalian intestinal and renal epithelia. Physiol Rev 2008;88(1):249–286.
6. Fafournoux P, Bruhat A, Jousse C. Amino acid regulation of gene expression. Biochem J 2000;351(Pt 1):1–12.
7. Kilberg MS, Pan YX, Chen H, Leung-Pineda V. Nutritional control of gene expression: how mammalian cells respond to amino acid limitation. Annu Rev Nutr 2005;25:59–85.
8. van Sluijters DA, Dubbelhuis PF, Blommaart EF, Meijer AJ. Amino-acid-dependent signal transduction. Biochem J 2000; 351(Pt 3):545–550.
9. Wilmore DW. The effect of glutamine supplementation in patients following elective surgery and accidental injury. J Nutr 2001;131(9 Suppl):2543S–2549S; discussion 2550S–2551S.
10. Angele MK, Nitsch SM, Hatz RA, et al. L-arginine: a unique amino acid for improving depressed wound immune function following hemorrhage. Eur Surg Res 2002;34(1-2):53–60.
11. Nicklin P, Bergman P, Zhang B, et al. Bidirectional transport of amino acids regulates mTOR and autophagy. Cell 2009; 136(3):521–534.
12. Walker V, Mills GA. Quantitative methods for amino acid analysis in biological fluids. Ann Clin Biochem 1995;32(Pt 1):28–57.
13. Puck A, Liappis N, Hildenbrand G. Ion exchange column chromatographic investigation of free amino acids in tears of healthy adults. Ophthalmic Res 1984;16(5):284–288.
14. ChenZhuo L, Murube J, Latorre A, del Rio RM. Different concentrations of amino acids in tears of normal and human dry eyes. Adv Exp Med Biol 2002;506(Pt A):617–621.
15. Deyl Z, Hyanek J, Horakova M. Profiling of amino acids in body fluids and tissues by means of liquid chromatography. J Chromatogr 1986;379:177–250.
16. Shimbo K, Oonuki T, Yahashi A, Hirayama K, Miyano H. Precolumn derivatization reagents for high-speed analysis of amines and amino acids in biological fluid using liquid chromatography/electrospray ionization tandem mass spectrometry. Rapid Commun Mass Spectrom 2009;23(10): 1483–1492.
17. Iwatani S, Van Dien S, Shimbo K, et al. Determination of metabolic flux changes during fed-batch cultivation from measurements of intracellular amino acids by LC-MS/MS. J Biotechnol 2007;128(1):93–111.
18. Shimbo K, Yahashi A, Hirayama K, Nakazawa M, Miyano H. Multifunctional and highly sensitive precolumn reagents for amino acids in liquid chromatography/tandem mass spectrometry. Anal Chem 2009;81(13):5172–5179.
19. Noguchi Y, Zhang QW, Sugimoto T, et al. Network analysis of plasma and tissue amino acids and the generation of an amino index for potential diagnostic use. Am J Clin Nutr 2006;83(2):513S–519S.
20. Tom A, Nair KS. Assessment of branched-chain amino acid status and potential for biomarkers. J Nutr 2006;136(1 Suppl):324S–330S.
21. Cynober LA. Plasma amino acid levels with a note on membrane transport: characteristics, regulation, and metabolic significance. Nutrition 2002;18(9):761–766.
22. Redmond HP, Stapleton PP, Neary P, Bouchier-Hayes D. Immunonutrition: the role of taurine. Nutrition 1998;14(7–8): 599–604.
23. Pasantes-Morales H, Wright CE, Gaull GE. Taurine protection of lymphoblastoid cells from iron-ascorbate induced damage. Biochem Pharmacol 1985;34(12):2205–2207.
24. Skrovanek S, Valenzano MC, Mullin JM. Restriction of sulfur-containing amino acids alters claudin composition and improves tight junction barrier function. Am J Physiol Regul Integr Comp Physiol 2007;293(3):R1046–1055.
25. Stapleton PP, O'Flaherty L, Redmond HP, Bouchier-Hayes DJ. Host defense—a role for the amino acid taurine? JPEN J Parenter Enteral Nutr 1998;22(1):42–48.
26. Windmueller HG, Spaeth AE. Respiratory fuels and nitrogen metabolism in vivo in small intestine of fed rats. Quantitative importance of glutamine, glutamate, and aspartate. J Biol Chem 1980;255(1):107–112.
27. Sakiyama T, Musch MW, Ropeleski MJ, Tsubouchi H, Chang EB. Glutamine increases autophagy under basal and stressed conditions in intestinal epithelial cells. Gastroenterology 2009;136(3):924–932.
28. Askanazi J, Carpentier YA, Michelsen CB, et al. Muscle and plasma amino acids following injury. Influence of intercurrent infection. Ann Surg 1980;192(1):78–85.
29. Parry-Billings M, Evans J, Calder PC, Newsholme EA. Does glutamine contribute to immunosuppression after major burns? Lancet 1990;336(8714):523–525.
30. Katragadda S, Talluri RS, Pal D, Mitra AK. Identification and characterization of a Na+-dependent neutral amino acid transporter, ASCT1, in rabbit corneal epithelial cell culture and rabbit cornea. Curr Eye Res 2005;30(11):989–1002.
31. Murata Y, Amao M, Hamuro J. Sequential conversion of the redox status of macrophages dictates the pathological progression of autoimmune diabetes. Eur J Immunol 2003;33(4): 1001–1011.
32. Murata Y, Yamashita A, Saito T, Sugamura K, Hamuro J. The conversion of redox status of peritoneal macrophages during pathological progression of spontaneous inflammatory bowel disease in Janus family tyrosine kinase 3(-/-) and IL-2 receptor gamma(-/-) mice. Int Immunol 2002;14(6):627–636.
33. Gordon S, Taylor PR. Monocyte and macrophage heterogeneity. Nat Rev Immunol 2005;5(12):953–964.
34. Mosser DM, Edwards JP. Exploring the full spectrum of macrophage activation. Nat Rev Immunol 2008;8(12):958–969.

Prevalence of and Risk Factors for Cornea Guttata in a Population-Based Study in a Southwestern Island of Japan

The Kumejima Study

Akiko Higa, MD; Hiroshi Sakai, MD; Shoichi Sawaguchi, MD; Aiko Iwase, MD; Atsuo Tomidokoro, MD; Shiro Amano, MD; Makoto Araie, MD

Objective: To examine the prevalence of and risk factors for cornea guttata in a rural southwestern island of Japan.

Design: Cross-sectional, population-based study. All residents of Kumejima Island, Japan, located in southwestern Japan (eastern longitude, 126° 48′; northern latitude, 26° 20′), 40 years or older were asked to undergo a comprehensive questionnaire and ocular examination, including noncontact specular microscopy of corneal endothelial cells. Of the 4632 residents, 3762 (81.2%) underwent the examination. The presence of guttata was determined when round or oval dark areas were observed in the specular microscopy images. Cornea guttata was graded from 0 to 4 depending on the total area of dark spots observed on the specular microscopy images. Diagnosis of primary cornea guttata was the main outcome measure.

Results: Of the 3060 eligible residents, 124 (4.1%; 95% confidence interval, 3.4%-4.8%) had cornea guttata in at least 1 eye. Logistic regression analysis with adjustment for age and/or sex indicated that older age, female sex, and thinner central corneal thickness were associated with an increased risk of cornea guttata.

Conclusions: The prevalence of cornea guttata is 4.1% among residents 40 years or older in Kumejima by specular microscopic criteria only, which is lower than the prevalence reported in the Reykjavik, Iceland, study. A higher prevalence may have been determined if slitlamp biomicroscopy findings had been included. Older age, female sex, and a thinner cornea were independently associated with a higher risk of cornea guttata.

Arch Ophthalmol. 2011;129(3):332-336

Author Affiliations:
Department of Ophthalmology, Faculty of Medicine, University of the Ryukyus, Okinawa, Japan (Drs Higa, Sakai, and Sawaguchi); Tajimi Iwase Eye Clinic, Gifu, Japan (Dr Iwase); and Department of Ophthalmology, University of Tokyo Graduate School of Medicine, Tokyo, Japan (Drs Tomidokoro, Amano, and Araie).

PRIMARY CENTRAL CORNEA GUTTATA is characterized by abnormal excrescences of collagenous basement membrane material produced by distressed endothelial cells in the central cornea. Excrescences are similar in appearance to the Hassall-Henle bodies that are observed in the peripheral cornea in older populations. Secondary guttata is a class of guttata that is associated with degenerative corneal disease, trauma, and inflammation and that usually disappears on removal of the cause.[1] Primary central cornea guttata, on the other hand, occasionally progresses to Fuchs corneal endothelial dystrophy with corneal endothelial decompensation.[1,2] Thus, primary central cornea guttata is a significant clinical sign of a predisposition for sight-threatening Fuchs corneal endothelial dystrophy.

Several studies have reported the prevalence of cornea guttata. A population-based study in Reykjavik, Iceland, reported that the prevalence of cornea guttata in 774 participants was 11% for female and 7% for male participants and that lower weight, lower body mass index, and a smoking history of longer than 20 pack-years were factors associated with a higher risk of cornea guttata.[3] Another study conducted in Japan and Singapore reported that the prevalence of cornea guttata in a non–population-based setting that included 299 Japanese and 465 Singaporeans 50 years or older was 3.7% in the Japanese and 6.7% in the Singaporeans.[4] A retrospective study in Japan found 4 patients with cornea guttata among 107 individuals ranging in age from 20 to 89 years.[5] Lorenzetti et al[6] reported a high prevalence of cornea guttata (31%-70%) in a hospital-based study in which participants ranging in age from 10 to 99 years underwent slitlamp examination. The present study was conducted to examine the prevalence of cornea guttata and associated factors of cornea guttata in a southwestern island of Japan.

Downloaded from www.archophthalmol.com on May 10, 2012
©2011 American Medical Association. All rights reserved.

METHODS

STUDY POPULATION

The prevalence of cornea guttata and its associated factors were examined as part of a population-based epidemiologic survey on ocular diseases in residents of Kumejima Island 40 years or older.[7] Kumejima is an island 63.2 km^2 located in the southwestern part of Japan (eastern longitude, 126° 48′; northern latitude, 26° 20′), west of the main island of Okinawa. It has a population of approximately 9000, with most residents originating from the Okinawa prefecture. The weather is warm and humid, with average daily temperatures of 22.7°C and an annual total rainfall of 2138 mm. This study was conducted from May 1, 2005, through August 31, 2006, and conformed to the tenets of the Declaration of Helsinki and the regional regulations approved by the regional council of Kumejima. According to the official household registration database, Kumejima had 5249 residents 40 years or older in 2005. After excluding residents who died, moved, or could not be located in Kumejima during the study period (n=617), 4632 residents were eligible for the study. All these residents were asked by letter and telephone to undergo the examinations held at the public hospital of Kumejima. Home visits and examinations were performed for inpatient, paralyzed, and disabled residents.

EXAMINATIONS

All participants provided written informed consent before the examinations. Body weight, height, and brachial blood pressure measurements were obtained, and a structured questionnaire was administered that included questions about self-reported main lifetime occupation (farming, fishing, office worker, service industry, housewife, and other), health history, surgery and trauma history, smoking (daily number of cigarettes and pack-years of smoking), history of outdoor work (farming, fishing and others and years of working), and use of hats and sunglasses.

A detailed ophthalmic examination was performed by experienced examiners and ophthalmologists and included uncorrected and best-corrected visual acuities, refraction, ophthalmoscopy, ocular fundus photography, visual field examination, and measurement of intraocular pressure (IOP), central corneal thickness (CCT), anterior chamber depth, and axial length of the eye. Slitlamp examination was not used to detect the presence of cornea guttata. Refraction was measured using an autorefractometer (ARK-730; Topcon Corporation, Tokyo, Japan). Intraocular pressure was measured 3 times using a Goldmann applanation tonometer under topical anesthesia, and the median value was adopted. Corneal endothelial cell morphology and CCT were examined with specular microscopy (SP-2000; Topcon Corporation). Measurement of CCT with this specular microscopy was confirmed to be highly correlated with measurement with ultrasonographic pachymetry in a previous study.[8] Anterior chamber depth and axial length of the eye were measured with a biometry system (IOL Master; Carl Zeiss Meditec, Dublin, California). Digital color fundus photographs (30° and 45°) were taken using a nonmydriatic ocular fundus camera system (Image Net TRC-NW7; Topcon Corporation). The examinations that did not require direct eye contact, including tests of refraction, visual acuity, specular microscopy, biometry, and fundus photography, were performed first. Measurement of IOP and gonioscopy were performed last.

When the participants could not visit the hospital, ophthalmologists visited their homes and performed the examinations, including IOP measurements with a portable tonometer (Perkins tonometer; Clement Clarke International Ltd, Harlow, England) or a handheld tonometer (Tonopen XL; Bio-Rad Laboratories, Hercules, California) and indirect and direct ophthalmoscopy (BS-II and BXα-13; Neitz, Tokyo). Because specular microscopy could not be performed on these participants, they were excluded from this analysis.

Only a specular microscope was used to detect cornea guttata because we thought that guttata at an early stage could be detected only with specular microscopy. The specular microscopic observation was performed in the area of approximately 0.4×0.2 mm at the central cornea, and the presence of guttata was determined by a masked examiner when round or oval dark areas were evident in the specular microscopy images. Owing to the large sample size, the specular microscopic observation was performed only at the central cornea. We used the modified grading method reported in the Reykjavik Eye Study[3] to grade cornea guttata from 0 to 4 on the basis of the ratio of the area of dark spots seen on the specular microscopy image to the entire area of the image, with 0 indicating no dark area; 1, less than 10%; 2, 10% to 25%; 3, 26% to 50%; and 4, more than 50%.

DATA ANALYSIS

All data were stored at the University of Ryukyus and University of Tokyo. Data analyses were performed using SPSS 15.0J for Windows statistical software (SPSS Japan Inc, Tokyo). Risk factors evaluated included sex, age, height, weight, diastolic and systolic blood pressure, diagnosis of diabetes or hypertension, smoking history, outdoor work history, self-reported main lifetime occupations, refractive error, CCT, IOP, and use of sunglasses, hat, prescription glasses, or contact lenses. Because age and sex were significantly associated with the presence of guttata in a preliminary analysis (data not shown), logistic analyses in which the explaining variables were each one of the listed risk factors and only sex (for the analysis of age), only age (for sex), and both age and sex (for the other risk factors) were included to adjust for age and/or sex. Data are expressed as mean (SD) unless otherwise specified.

RESULTS

Of the 4632 eligible residents, 3762 (81.2%) underwent the examination. The 3762 participants were younger than the 870 nonparticipants (mean age, 59.1 [14.9] vs 61.8 [14.0] years; $P<.001$, unpaired t test), and more women were among the participants (male to female ratio, 1833: 1929 vs 555:315; $P<.001$, χ^2 test).

Of the 7524 eyes (3762 participants), 872 right eyes and 895 left eyes were excluded for various reasons, including history of intraocular surgery and difficulties in obtaining clear images of corneal endothelial cells with specular microscopy (**Table 1**). Diseases that can affect the corneal endothelium, such as iridocorneal endothelial syndrome, were not observed in any of the participants. Thus, 2890 right eyes and 2867 left eyes were included in the current analysis. At least 1 eye was eligible in 3060 residents, and both eyes were eligible in 2714. Among the 3060 included residents, more were men (50.7% vs 49.3%; $P<.001$, χ^2 test) and younger (mean age, 59.2 [12.9] vs 73.3 [12.7] years; $P<.001$, unpaired t test) than among the 702 excluded individuals. Of the 3060 eligible residents, 124 (4.1%; 95% confidence interval, 3.4%-4.8%) had cornea guttata in at least 1 eye,

Downloaded from www.archophthalmol.com on May 10, 2012
©2011 American Medical Association. All rights reserved.